DOI: 10.1002/ ((please add manuscript number))
Article type: Review

Multifunctional coatings and nanotopographies: towards cell instructive and antibacterial implants

Carlos Mas-Moruno, Bo Su and Matthew J. Dalby*

Dr. C. Mas-Moruno
Biomaterials, Biomechanics and Tissue Engineering Group, Department of Materials Science and Engineering & Center in Multiscale Science and Engineering, Universitat Politècnica de Catalunya (UPC), Barcelona, 08019, Spain
E-mail: carles.mas.moruno@upc.edu

Prof. Dr. B. Su
Bristol Dental School, University of Bristol, Bristol, BS1 2LY, United Kingdom.

Prof. Dr. M. J. Dalby
Centre for Cell Engineering, University of Glasgow, Glasgow, G12, Scotland, United Kingdom.

Keywords: implant coatings, osseointegration, infection, nanotopographies, multifunctional coatings

Abstract: In biomaterials science, it is nowadays well accepted that improving the biointegration of dental and orthopedic implants with surrounding tissues is a major goal. However, implant surfaces that support osteointegration may also favor colonization of bacterial cells. Infection of biomaterials and subsequent biofilm formation can have devastating effects and reduce patient quality of life, representing an emerging concern in healthcare. Conversely, efforts towards inhibiting bacterial colonization may impair biomaterial-tissue integration. Therefore, to improve the long-term success of medical implants, biomaterial surfaces should ideally discourage the attachment of bacteria without affecting eukaryotic cell functions. However, most current strategies seldom investigate a combined goal. This work reviews recent strategies of surface modification to simultaneously address implant biointegration while mitigating bacterial infections. To this end, two emerging solutions are considered, multifunctional chemical coatings and nanotopographical features.

1. Introduction

The replacement and healing of non-functional tissues has become a major challenge worldwide, due to the increase in life expectancy and the prevalence of age-related diseases. In the case of osteoarticular conditions, > 1 million total knee and hip replacement surgeries were performed in 2010 in the United States,[1,2] and projections indicate that the number of primary and revision joint arthroplasties will grow significantly in coming years;[3] similar statistics are also found in Europe.[4,5] However, and despite the intrinsic capacity of bone to regenerate after injury, complete fracture healing and implant fixation are not always possible. [6,7] Thus, joint replacements still fail at unacceptable rates, with some reports describing revision rates as high as 17.5% for total hip arthroplasty.[8]

Successful implant fixation and full recovery of lost function depend on many factors, which include patient characteristics (e.g. age, alcohol consumption, smoking habits, metabolic conditions), factors associated with the implantation site (e.g. injury and infection at the site, poor vascularization) and those related to the surgical procedure and implant properties.[9] Nonetheless, it is increasingly accepted that the two major causes of implant failure are aseptic loosening and infection.[10] For example, a recent epidemiologic study indicates that mechanical loosening (20.3%) and infection (20.4%) were the most common etiology for revision of total knee arthroplasty in the United States between 2009 and 2013.[11]

Incomplete osteointegration (i.e. not achieving a strong and durable connection between periimplant bone and the implant surface)[12] represents a major contribution towards aseptic loosening. Although Brånemark's description of osteointegration originally referred to titanium (Ti) dental implants, it is nowadays widely used for orthopedic implants as well. Osteointegration relies on i) mechanical interdigitation, which ensures the primary fixation of the implant with bone after surgery, and ii) cellular interactions at the surface level, which are responsible of promoting osteoconduction, osteoinduction and healing during the first 3-4 months.[13] Both processes are crucial to ensure an optimal clinical outcome, i.e. bone healing, allowing the recovery of lost function and patient's mobility.

Implant infection also represents a major concern.[14,15] In fact, post-implantation, patients are more susceptible to infection. This increased vulnerability relates to the fact that the efficacy of the immune system is locally reduced by the presence of a foreign body (e.g. a metallic implant) and to the predilection of bacteria to adhere to solid substrates.[16] Thus, it only takes a few adherent bacteria to attach to the implant surface, grow and multiply to form a biofilm.[17,18] This process is usually initiated by planktonic bacteria, which act as primary colonizers, and is followed by a second phase, in which

secondary (or late) colonizers are irreversibly bound to the surface and create a biofilm. Once established, biofilms are highly resistant to the immune system and conventional drugs, such as antibiotics, and may also spread and infect other tissues. This further affects patient morbidity and even results in death in severe cases.[19,20,21,22] Moreover, the emergence of antibiotic resistance, e.g. methicillin-resistant *Staphylococcus aureus* (MRSA), poses a serious threat.[14,19,23] Although the numbers vary greatly depending on the surgical procedure and the type of device, infection of orthopedic implants may occur in up to 5% of cases.[9] In the case of dental implants, infection rates are higher, reaching values of peri-implantitis or dental implant infections as high as 14%.[24]

It is therefore not surprising that extensive research is being performed to tackle these two problems, and a large number of strategies for surface modification have been described to either improve implant osteointegration[9,13,25,26,27,28,29] or reduce bacterial infection.[9,14,24,30,31,32,33,34] However, the necessity of simultaneously addressing both these limitations has only been highlighted recently.[10,35,36,37]

The development of multifunctional strategies that promote osteointegration while mitigating bacterial colonization is clearly important because both effects are necessary to ensure an optimal, long-term functionality of medical implants. However, we note that this notion is not new. Already in the late 1980s, the attachment of host cells and bacteria to the implant surface was defined as a competitive "race for the surface".[38] In such a scenario, the winner takes it all. If host eukaryotic cells colonize the implant and proliferate faster, the resulting adherent cell layer will discourage bacterial attachment and reduce the risk of infection. In contrast, if bacteria are able to adhere and produce biofilms, the osteointegration of the implant will be seriously compromised.

Further, classical approaches focusing only on improving one biological effect might paradoxically be detrimental for the other. Implant surfaces that promote osteointegration (e.g. rough surfaces) may also facilitate an increased bacterial attachment. Conversely, bactericidal agents used to inhibit bacterial infection may be toxic or impair normal host cell functions.[9,10]

The aim of this review is to provide an overview of the existing strategies of surface modification that simultaneously combine cell adhesive/osteoinductive and antibacterial properties. Implants with such multifunctional potential would accelerate implant osteointegration and healing but minimize the risk of early/late infections – thus improving their clinical outcome and reducing the number of revision surgeries. To this end, this review particularly focuses on two emerging solutions, the use of multifunctional chemical coatings and nanotopographical features.

2. Classical strategies and limitations

2.1. Strategies to improve osteointegration

Improvement of the implant's bioactivity towards enhanced levels of osteointegration has been classically addressed by physical and chemical methods of surface modification (Figure 1A), and several reviews comprehensively covering these approaches are available.[9,13,25,26,27,28,29]

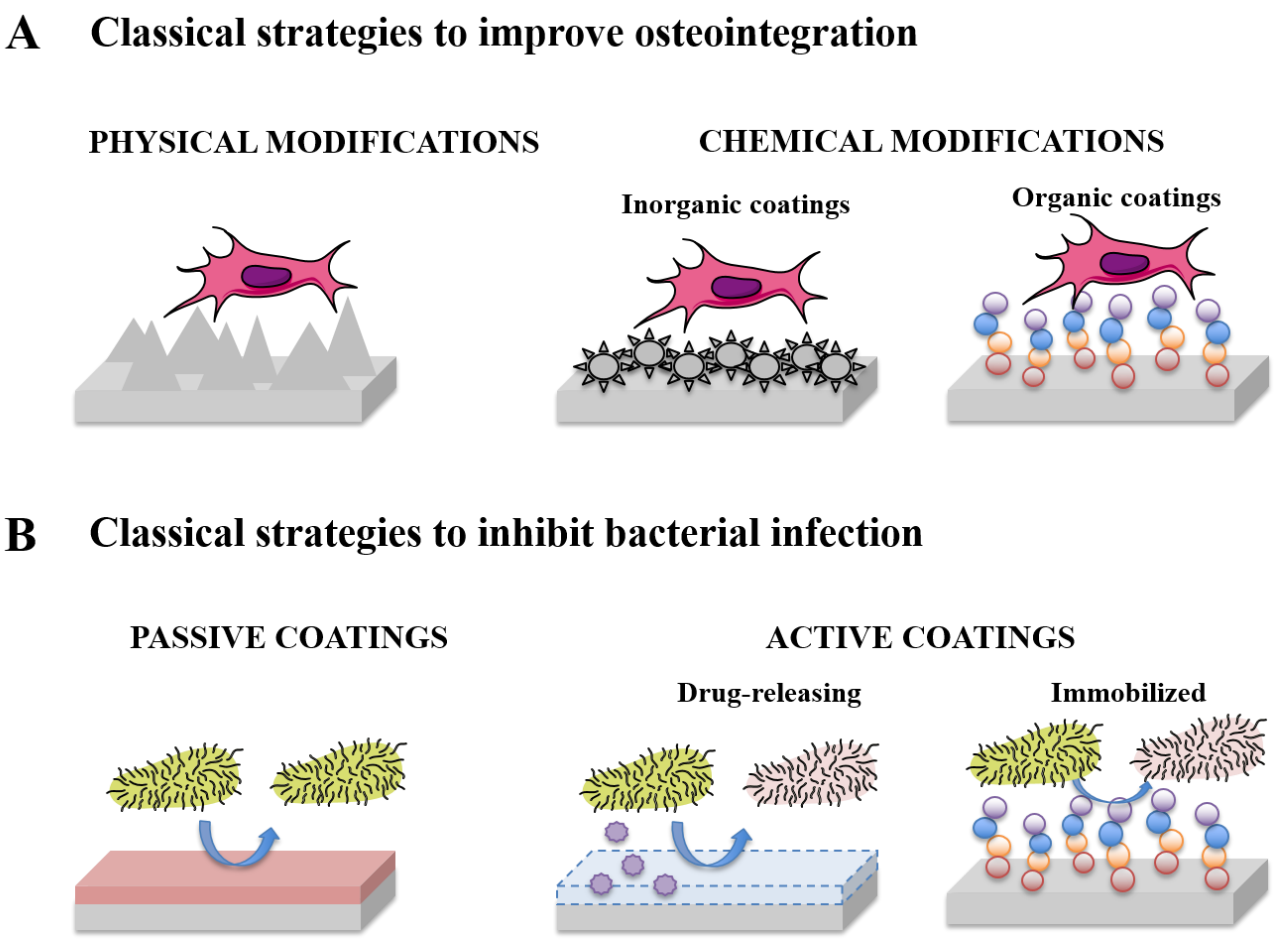

Figure 1: Schematic summary of classical strategies of surface functionalization. A) Improvement of osteointegration can be achieved by physical methods, which commonly focus on modifying the surface topography (e.g. surface roughness), or chemical methods, which are based on inorganic (e.g. calcium phosphate) or organic (e.g. peptide and protein) coatings. B) The strategies to inhibit bacterial infection can be divided into passive (e.g. anti-adhesive) or active (e.g. drug eluting or immobilized) coatings.

Physical methods have largely focused on increasing the average roughness (Ra) of the implant surface, following experimental evidence *in vivo* that substrates with higher Ra were capable of achieving higher rates of osteointegration.[13,39] This observation may be due to higher micromechanical retention of bone on rougher substrates compared to smooth ones, and the positive influence of surface

roughness on protein adsorption and osteoblastic function.[40,41,42] Increasing surface roughness at the submillimeter – micrometer level can be easily achieved by several inexpensive methods, such as grit blasting or acid etching, and many dental implants nowadays display Ra values within 1 to 5 µm. The main limitation of non-specifically increasing the surface roughness of an implant above a certain threshold (some authors have defined this value as Ra > 0.2 µm)[43,44] is that such rougher surface will likely support higher levels of bacterial attachment as well (Table 1). Alternatively, well-defined surface modifications at the nanotopographic level have emerged – and are now established – as a feasible way to control stem cell response and osteogenic differentiation. Topographical features at the nanoscale are not expected to promote bacterial attachment (i.e. they are below 0.2 µm) and can be tuned to even prevent infection. This subject will be covered with detail in Sections 4 and 5 of this review.

Chemical coatings generally try to mimic the extracellular matrix (ECM) of bone.[27] As such, inorganic coatings are often based on calcium phosphate (CaP) / hydroxyapatite (HAp), the mineral component of bone. Organic coatings, on the other hand, include cell adhesive proteins or peptides derived from the ECM. The deposition of CaP minerals to bioactivate implant surfaces has represented a main focus of research for more than 30 years now.[45,46] This was originally achieved by plasma spray and electrodeposition methods,[47,48] but concerns on the (poor) mechanical stability of thick CaP coatings were later reported.[49,50] To overcome this, biomimetic strategies were described during the 90s. In general, these strategies allowed the formation of thinner CaP layers, exhibiting high bioactivity and better mechanical properties.[51,52,53,54,55,56,57] A representative and successful example is the method developed by Kokubo,[51,58] which combines a basic etching and a thermal treatment of Ti to produce an amorphous sodium titanate layer. Immersion of treated surfaces into physiological buffers (i.e. simulated body fluid, SBF) drives the nucleation of bone-like apatite, thus conferring bioactivity to the material. Interestingly, this method has shown good versatility and can be applied to other medically-relevant materials, including niobium, tantalum and zirconium.[59,60,61]

These coatings are highly osteoconductive and have shown osteointegrative potential *in vivo*.[9,13] According to some authors, CaP materials are osteoinductive as well, which may be attributed to their capacity to adsorb proteins such as growth factors (GFs). In this regard, both their chemistry and specific surface area can be tuned to efficiently immobilize bone morphogenetic proteins (BMPs) – yet it is plausible that these characteristics (i.e. high specific surface area) may concomitantly favor bacterial adhesion (Table 1).[62] A potential solution to that is to use CaP coatings as drug delivery systems (e.g. loaded with antibacterial agents),[63] so the bioactivity of CaP can be combined with antibacterial properties (this strategy will be discussed in Section 3.2).

Organic coatings include a diverse range of molecules, from polymers to proteins, peptides or small organic molecules. [13,64] In general, this strategy has focused on proteins from bone ECM, with fibronectin, vitronectin and collagens being representative examples.[27,28,65] The majority of ECM proteins support cell attachment via cell adhesive motifs such as the RGD sequence,[66,67] which recognizes and binds to integrin receptors expressed by eukaryotic cells.[68] Integrin (and non-integrin) binding ligands have thus been frequently used not only to improve cell adhesion but also to stimulate cell proliferation and differentiation.[69,70] As the use of native ECM proteins and synthetic peptides entails limitations of stability, biological potency and specificity (these issues still remain controversial),[71,72,73] advances in this field have focused on recombinant protein fragments,[74,75,76,77] multifunctional peptides[78,79,80] and non-peptidic ligands.[69,81]

Inducing integrin signaling cascades has become a common strategy to improve bone healing. However, to optimally mimic the cellular microenvironment on the biomaterial surface, signaling through other mechanisms is required. For instance, several GFs such as BMPs[82] are known to cooperate with integrin ligands to regulate bone regeneration. In this regard, a growing body of evidence indicates that GF signaling can be regulated and enhanced by dynamic crosstalk with integrin receptors.[83,84,85] In particular, recent examples have shown that the combination of ECM proteins with BMPs has a synergistic effect to induce stronger osteogenic signals and bone formation *in vivo* with reduced doses of GF.[86,87,88,89] These approaches are of relevance and constitute a hot topic of research, as they take advantage of the osteoinductive potential of BMPs while overcoming the complications and concerns associated to their use.[90, 91] Further information is available in the recent literature.[35,84,85]

Functionalization of medical implants with molecules from the ECM appears to provide a strategy that should not promote bacterial colonization. However, organic coatings are not exempt from risks either. For example, the production of proteins (or fragments) by recombinant methods is commonly done using bacterial systems. Such methods inherently entail the risk of introducing remnants of bacteria (e.g. endotoxins) on the biomaterial surface during the coating procedure. In addition, bacteria share similar adhesion mechanisms with eukaryotic cells to attach to surfaces, and may bind to ECM proteins such as fibronectin[92,93] or collagens[94].

Finally, it should be mentioned that the aforementioned strategies (e.g. surface roughness and bioactive coatings) can be combined to achieve synergistic effects and improved biological responses. For example, grit blasting of titanium surfaces,[95] followed by alkaline etching and thermal treatments (a method named *2Step*) showed accelerated *in vitro* formation of bioactive apatite on the bottom of the topographical valleys in comparison to smooth surfaces.[96] This treatment showed improved

differentiation of human osteoblastic cells *in vitro*[97] and enhanced bone formation in vivo.[13,98] Another study evaluated the combination of different levels of surface roughness with a cyclic RGD peptide. Interestingly, the highest levels of cell adhesion were obtained on the rougher surfaces functionalized with the peptide, compared to peptide-coated smooth surfaces or non-functionalized controls (smooth and rough).[99]

2.2. Strategies to inhibit bacterial infection

The number of strategies investigated to fight bacterial infection is also growing, and this field represents a very active area of research in the biomaterials community.[9,14,24,30,31,32,33,34] Although a myriad of methods have been described, a common classification is to divide antibacterial treatments as passive or active, depending on their ability to discourage bacterial cell attachment or actually kill contaminating bacteria, respectively. Active coatings may rely on the release of antibacterial agents (release-based) or surface strategies (non-release-based) (Figure 1B). Regardless of classification, the goal is always the same: inhibit bacterial adhesion on the surface and prevent the formation of highly resistant biofilms.

Passive coatings are typically based on anti-adhesive polymers that prevent protein and cellular (e.g. bacteria) attachment. Alternatively, such anti-fouling effect can also be achieved using nanotopographies (see Section 5.1). Among all polymers, polyethylene glycol (PEG) is probably the most widely used to confer anti-fouling properties to a material surface.[30,100] Its repelling properties are related to its flexible and hydrophilic chains. These chains form a wide exclusion volume that blocks protein adsorption and cell attachment. Other examples of low fouling polymers include poly(methacrylic acid) (PMAA), dextran or hyaluronic acid.[36] Such coatings can easily be applied to a broad range of materials and have the advantage of being simple, effective and not requiring the use of drugs. However, the main strength of anti-adhesive coatings represents a concomitant weakness, as very efficient bacteria repelling coatings will inhibit eukaryotic cell attachment as well. For this reason, anti-fouling polymers often require the incorporation of cell adhesive sequences to preserve cell adhesion and the biomaterial's functionality. Such strategy represents a clear example of multifunctional coating and is described later in Section 3.1.

In contrast to passive coatings, active coatings exert their antibacterial action by directly killing bacteria. This may be achieved by a very diverse range of molecules, including bactericidal polymers (e.g. chitosan, cationic polymers), quaternary ammonium salts, ions (e.g. silver, zinc), antibiotics, bactericidal agents (e.g. chlorhexidine) and antimicrobial peptides (AMPs).[9,14,24,31,32,33,34] These strategies are largely reliant upon two physicochemical approaches: i) the incorporation of antibacterial

agents (e.g. antibiotics or silver ions) on the biomaterial via physical adsorption or entrapment in polymeric matrices (drug-releasing mechanism), and ii) the covalent functionalization of the materials with bactericidal molecules (e.g. AMPs). Although drug-releasing approaches are commonly applied and have proven their efficacy in many reports, the second approach (i.e. immobilization of the antibacterial molecule) warrants further research because the release of antibacterial agents entails several risks in terms of (off target) toxicity, rapid dwindling concentration due to release and loss of activity over time; these latter effects necessitate use of very high doses increasing toxicity and increasing probability of bacterial resistance.

In particular, the emergence of antimicrobial resistance mechanisms in bacteria severely compromises the use of antibiotics and other antibacterial drugs.[101,102] For instance, the highly virulent multi-drug resistant strains of *Staphylococcus aureus* (e.g. MRSA) establish dangerous infections that in many instances are very difficult or impossible to treat with existing medicines.[103] These bacteria, also known as "superbugs", are considered one of the most frequent causes of healthcare-associated infections worldwide and are responsible for a high mortality rate. As mentioned before, on biomaterial-associated infections, the picture is further complicated by the growth of biofilms, exacerbating the antibiotic resistance scenario. Furthermore, it has also been described that the release of antibacterial agents such as silver or antibiotics may negatively affect osteoblastic functions as well (Table 1). [104,105]

Table 1. Summary of classical strategies of surface functionalization of biomaterials, main effect targeted and potential non-wanted effects.

Strategy	Main effect targeted	Limitation
Increasing surface roughness (e.g. Ra in the µm range)	Improvement of osteointegration by higher mechanical retention	Rough surfaces (e.g. > 0.2 µm) may also increase bacterial attachment
Inorganic coatings based on CaP / bone-like apatite	Providing osteoconductive / osteoinductive potential to improve osteointegration	Higher specific surface area of CaP may also increase bacterial attachment
Organic coatings based on proteins / peptides from the ECM	Providing osteoconductive / osteoinductive potential to improve osteointegration	Bacteria share cell adhesion mechanisms with eukaryotic cells (using ECM molecules)
Anti-adhesive coatings	Inhibiting / repelling bacterial attachment	Eukaryotic cell attachment is also compromised (inhibited)
Bactericidal coatings (release-based and non-release-based)	Killing bacteria / inhibiting bacterial attachment	Eukaryotic cell attachment, functions and viability may be also compromised

3. Multifunctional chemical coatings

The functionality of biomaterials can be significantly improved by either enhancing their interaction with eukaryotic cells (e.g. osteoblasts – improved osteointegration) or inhibiting bacterial infection. However, specifically improving host cell adhesion while inhibiting bacterial attachment is a challenging task. As a matter of fact, most approaches intended to confer osteoinductive properties to biomaterials have not considered the risk of bacterial colonization. Or worse, treatments or surface modifications that facilitate cell adhesion and proliferation, may also favor bacterial attachment and biofilm formation. Conversely, research efforts devoted to inhibit bacterial colonization are often related to anti-adhesive polymers or cytotoxic agents that may compromise osteoblast-like cell functions.

In this section, we will focus on coatings composed of distinct chemical entities (e.g. materials, biomolecules or drugs), which are combined in a way that a dual function (i.e. osteointegrative and antibacterial) is achieved. These strategies are normally not intended to modify the properties of the bulk material, only its surface, and hence are categorized as strategies of surface functionalization. Although the number of examples in the literature is rapidly increasing and a myriad of combinations are possible, we will center this section according to three differentiated approaches: i) antibacterial coatings functionalized with cell instructive molecules; ii) osteoconductive/osteoinductive coatings loaded with antibacterial agents; and iii) immobilized multifunctional peptides (Figure 2 and Table 2).

3.1 Coatings based on antibacterial polymers

3.1.1 Functionalized anti-adhesive polymers

The first approach to achieve cell instructive and antibacterial effects focuses on the use of anti-fouling polymers functionalized with cell adhesive peptides (Figure 2A). It is plausible that this strategy was originally not conceived as a multifunctional coating, but that it responded to the inherent limitations of anti-fouling polymers like PEG. As previously outlined, PEG is very efficient in preventing bacterial attachment, but it also blocks the adhesion of wanted host cells – as a matter of fact, PEG is frequently used to reduce non-specific cell binding in cellular and biophysical studies. Thus, the incorporation of a cell adhesive sequence such as RGD is required to maintain cell-binding properties.

To the best of our knowledge, the first report following this strategy was published by Harris and coworkers in 2004 (Table 2).[106] In this work, PEG was electrostatically adsorbed on Ti surfaces using poly-L-lysine (PLL), and the PEG-PLL co-polymer was further functionalized with an RGD peptide using vinyl sulfone-thiol chemistry. The PEG coating significantly reduced the attachment of *Staphylococcus aureus*, and, of note, the presence of the RGD peptide did not affect the antibacterial

activity. In a subsequent study, the same group showed a reduced attachment of other medically relevant bacterial strains (e.g. *Staphylococcus epidermidis*, *Streptococcus mutans* and *Pseudomonas aeruginosa*).[107] However, the authors did not check the response of eukaryotic cells to the RGD peptide on these studies. Both effects were actually reported in other investigations, which reflected the multifunctional potential of this strategy: the passive PEG layer inhibited bacterial attachment, while the RGD peptide simultaneously supported (or improved) osteoblast (OB)[108] or fibroblast (FB)[109] adhesion. In addition to electrostatic adsorption, a number of other methods have been proposed to coat Ti surfaces with PEG, such as electrodeposition, silanization and plasma polymerization.[109]

This technique is facile and versatile, as it can be expanded using different anti-fouling polymers and bioactive sequences. For instance, PMAA, dextran or hyaluronic acid have been combined with cell adhesive sequences (e.g. RGD, silk sericin) or GFs (e.g. BMP-2, vascular endothelial growth factor, VEGF) demonstrating excellent dual potential (see Table 2 for details).[110, 111,112]

Recent studies have further combined the anti-adhesive properties of PEG and other polymers with bactericidal agents (e.g. quaternary ammonium compounds, ions, AMPs or bactericidal polymers) to simultaneously exploit passive and active antibacterial mechanisms. [113,114,115,116,117,118,119] Such dual antibacterial function aims at both preventing bacterial attachment and killing bacteria able to adhere. This approach is also interesting because it inhibits the accumulation of bacterial debris and proteins, which may provide anchoring points for the formation of biofilms. These works, however, do not address eukaryotic cell adhesion – crucial to ensure implant integration with tissues – and will not be covered in this review.

The major limitation of using polymers to coat substrates is the risk of polymer degradation over time. Degradation may compromise the long-term stability and prolonged effect of the coatings. Moreover, their fabrication and obtaining of defined and homogenous structures may be challenging.

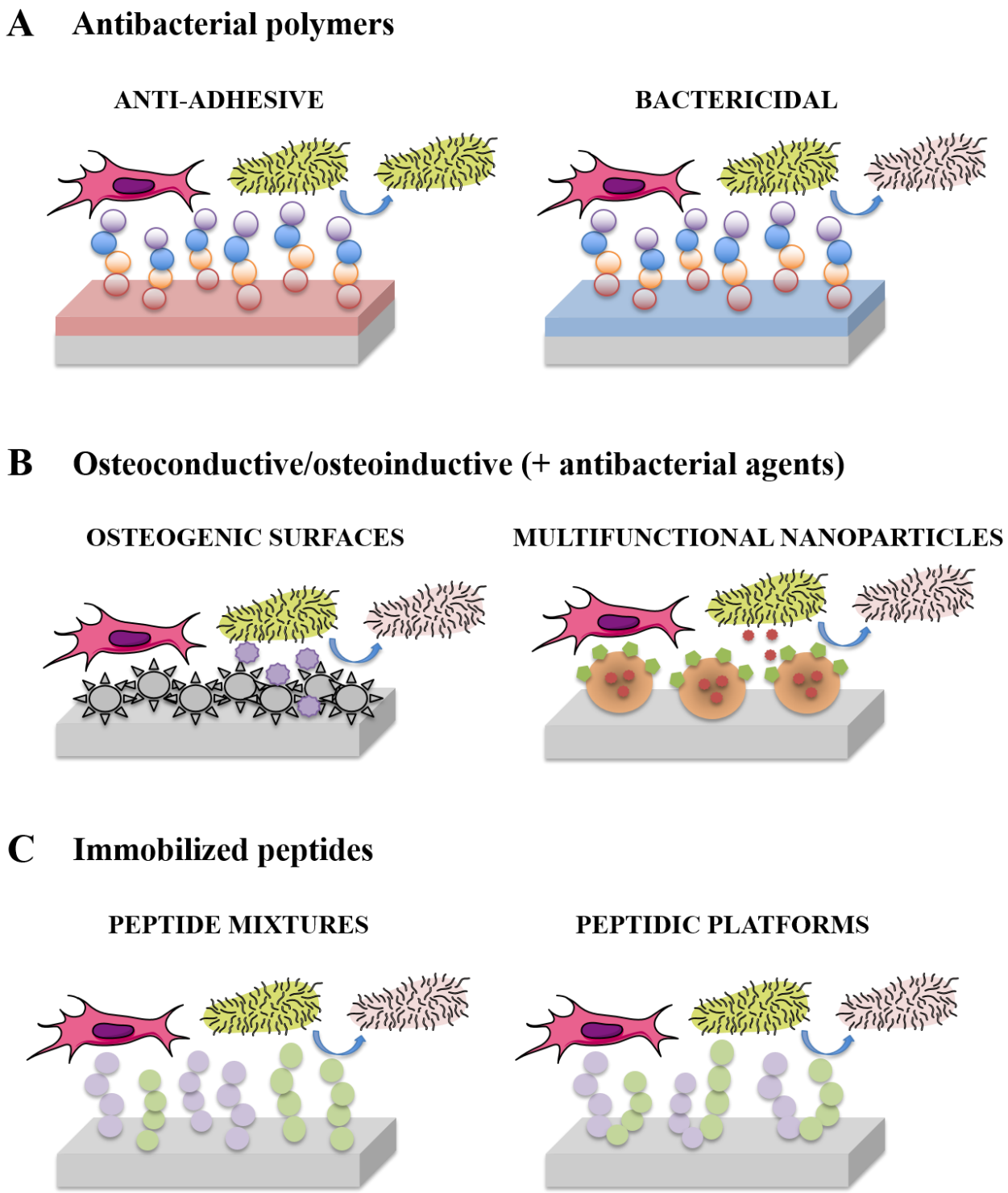

Figure 2: Schematic summary of multifunctional strategies to achieve both cell instructive and antibacterial properties. A) Antibacterial polymers can be used to either repel (anti-adhesive, e.g. PEG) or kill (bactericidal, e.g. chitosan) bacteria; in both cases the presence of a cell adhesive sequence is required; B) the opposite approach is to use osteogenic surfaces (Ti dioxide nanotubes, TNTs, CaP coatings) or RGD-decorated nanoparticles that incorporate and release antibacterial agents (e.g. antibiotics, silver, AMPs); C) A third strategy is to covalently immobilize cell adhesive sequences and AMPs on the biomaterial surfaces. To this end, peptide mixtures or peptidic branched platforms can be used.

3.1.2 Functionalized bactericidal polymers

An alternative strategy to anti-adhesive coatings like PEG is to use polymeric coatings that are directly bactericidal. One canonical example is chitosan, which is well known for its antibacterial properties.[120] Although this polymer has been also attributed with good biocompatibility and cell adhesive activity, several reports have combined chitosan with cell adhesive peptides to achieve a dual effect; examples are provided in Table 2. For instance, Neoh and colleagues adsorbed polyelectrolyte multilayers of chitosan and hyaluronic acid on Ti, and anchored an RGD peptide to the external chitosan layer via carbodiimide chemistry. The resulting surfaces inhibited *Staphylococcus aureus* adhesion while improving osteoblastic responses (adhesion, proliferation and alkaline phosphatase, ALP, activity).[121] In a parallel study, the same authors reported the covalent immobilization of RGD-coated chitosan with very similar biological results.[122] In this case, Ti was sequentially modified with dopamine (which binds to Ti via the catechol moiety) and glutaraldehyde, rendering a free aldehyde group on the surface that was used to covalently bind chitosan by reductive amination. The RGD sequence was finally grafted using carbodiimide chemistry. Another viable solution is to immobilize GFs or enzymes onto chitosan layers to improve cell adhesion and also osteogenic differentiation. This has been achieved combining chitosan or carboxymethyl chitosan with BMP-2[123,124], VEGF[112] or ALP[125] (see Table 2 for details). The biological potential of chitosan can be further increased with other antibacterial agents. In a recent study, the combination of chitosan with gallium effectively decreased *Escherichia coli* and *Pseudomonas aeruginosa* viability. Interestingly, gallium also showed a beneficial osteogenic effect.[126]

In addition to chitosan, a number of other antibacterial cationic polymers have been described, such as ε-poly-L-lysine (ε-PLL), quaternary ammonium polymers, polyethylenimine and polyguanidines.[127] Among them, ε-PLL has shown a broad spectrum of antimicrobial activity against Gram-negative and Gram-positive bacteria but low toxicity for eukaryotic cells.[127,128] Taking advantage of this, ε-PLL-based hydrogels with wound healing and anti-infective properties have been developed.[129,130] As positively charged polymers easily adsorb electrostatically on oxidized metallic surfaces, it is expected that these polymers may also be used as multifunctional coatings on orthopedic implants.

3.2 Osteoconductive/osteoinductive surfaces loaded with antibacterial agents

A conceptually similar but inverse approach is to use surfaces that have osteoconductive or osteoinductive potential. Coatings such as Ti dioxide nanotubes (TNTs) or CaP can be doped with antibacterial agents, such as antibiotics or cations.

TNTs represent a very attractive strategy in the biomedical field as they have excellent corrosion resistance and biocompatibility. In particular, they have been described to improve osteoblastic functions and, in some cases, have antibacterial potential (although these effects are largely reliant on the TNTs geometry and physicochemical properties).[131] On the basis of these interesting features, TNTs have been fabricated by different methods (e.g. template-assisted, anodization or hydrothermally) and loaded with silver (either as ion[132] or nanoparticles[133,134]), zinc[135,136], copper[137] or antibiotics.[138,139] Overall, this approach has shown good biocompatibility with OB-like cells, improved osteogenic responses and reduced adhesion and viability of several bacterial strains (Table 2). For this type of system, a crucial parameter to control is the concentration of the molecule released, as it has been observed that the release of high concentrations of silver may be cytotoxic for several eukaryotic cell types (e.g. epithelial cells, FBs and OBs),[133,140] and that high doses of ZnO and silver nanoparticles may decrease the antibacterial activity or even promote bacterial attachment.[141] Moreover, recent evidence has shown that certain bacterial isolates may develop resistance to silver.[142] Alternatively, TNTs can be engineered in a way that support the adhesion of osteogenic cells but reduce bacterial attachment without the addition of ions (see Section 6 for details).[143,144]

A more classical approach would be to employ CaP coatings, which are inherently osteoconductive, and load them with antibacterial agents. Here, silver is frequently used too.[145,146,147,148,149] For example, HAp coatings doped with Ag_2O and SrO were plasma-sprayed onto Ti to incorporate bactericidal potential to the inorganic substrate. Interestingly, silver was highly effective against *Pseudomonas aeruginosa* but the release of this ion was detrimental for the activity of OBs. Co-doping the coating with SrO seemed to compensate this negative effect and rescued normal osteoblastic functions (Table 2).[150] Thus, the antibacterial potential of silver can be combined with the bioactivity of strontium within CaP-based coatings to improve Ti implants response; recent reports have further exploited such interesting multifunctional approach.[151,152] The limitations described for silver in the previous examples can be circumvented using other antibacterial agents. For example, AMPs (HHC36: KRWWKWWRR; Tet213: KRWWKWWRRC) have been incorporated into CaP coatings.[153,154] While Tet213 showed toxicity for OB-like cells even at low concentrations, HHC36 displayed little toxicity. HHC36-CaP-coated Ti surfaces showed antibacterial potential against *Staphylococcus aureus*

and *Pseudomonas aeruginosa* and improved levels of osteoconductivity in an *in vivo* model of trabecular bone growth using cylindrical implants in rabbits.[154] This study suggests that AMPs may be a good alternative to silver but also shows that the selection of the peptide is important (i.e. balancing good antibacterial activity with low toxicity for eukaryotic cells). Antibiotics have also been frequently combined with CaP coatings showing effective osteoconductivity and antibacterial properties.[63] Diverse examples of this strategy can be found in the literature and include the use of gentamicin,[155] vancomycin[156,157] and its derivatives,[158] among others.

Regardless of the antibacterial agent used, a common limitation of this approach is the burst release of the bactericide. Such rapid release may be deleterious for several reasons, i) it reduces the long-term effectiveness of the coatings; ii) a high concentration of drug may be toxic for host cells; and iii) it may promote bacterial resistance. A potential solution to this problem is to introduce polymeric coatings that cap and protect the coating, and that deliver the drug as they degrade, thus slowing down release kinetics. For example, this has been achieved with polylactic-*co*-glycolic acid (PLGA), which was used to control the delivery of the antibiotic clindamycin from different CaP coatings.[159] A similar polymeric coating was used to fine-tune the release of drugs from TNTs.[138] In this case, TNTs were loaded with gentamicin and subsequently covered by PLGA and chitosan coatings (Figure 3).[138] Interestingly, the polymeric coatings not only improved the drug-release kinetics (i.e. decreased burst release) but also enhanced OB-like cell adhesion and reduced bacterial viability, representing an elegant example of tri-functional coating (e.g. TNT + antibiotic + chitosan). Similarly, the release of an AMP from a TNT-CaP coating was tuned using a phospholipid (1-palmitoyl-2-oleoyl-sn-glycero-3-phosphocholine, POPC) capping layer.[160] Regulating the delivery of drugs from biomaterials with polymeric coatings is not easy and depends on many factors (e.g. the degradability of the polymer and stability, its chemistry, the number of layers deposited…) but opens new avenues to finely control the antibacterial action, ensuring prolonged effects and reducing unspecific toxicity. As new methods become available, a higher control might be possible. One of such methods is plasma polymerization, which has recently shown to be very effective in tuning the release of antibiotics from different biomaterials.[161,162]

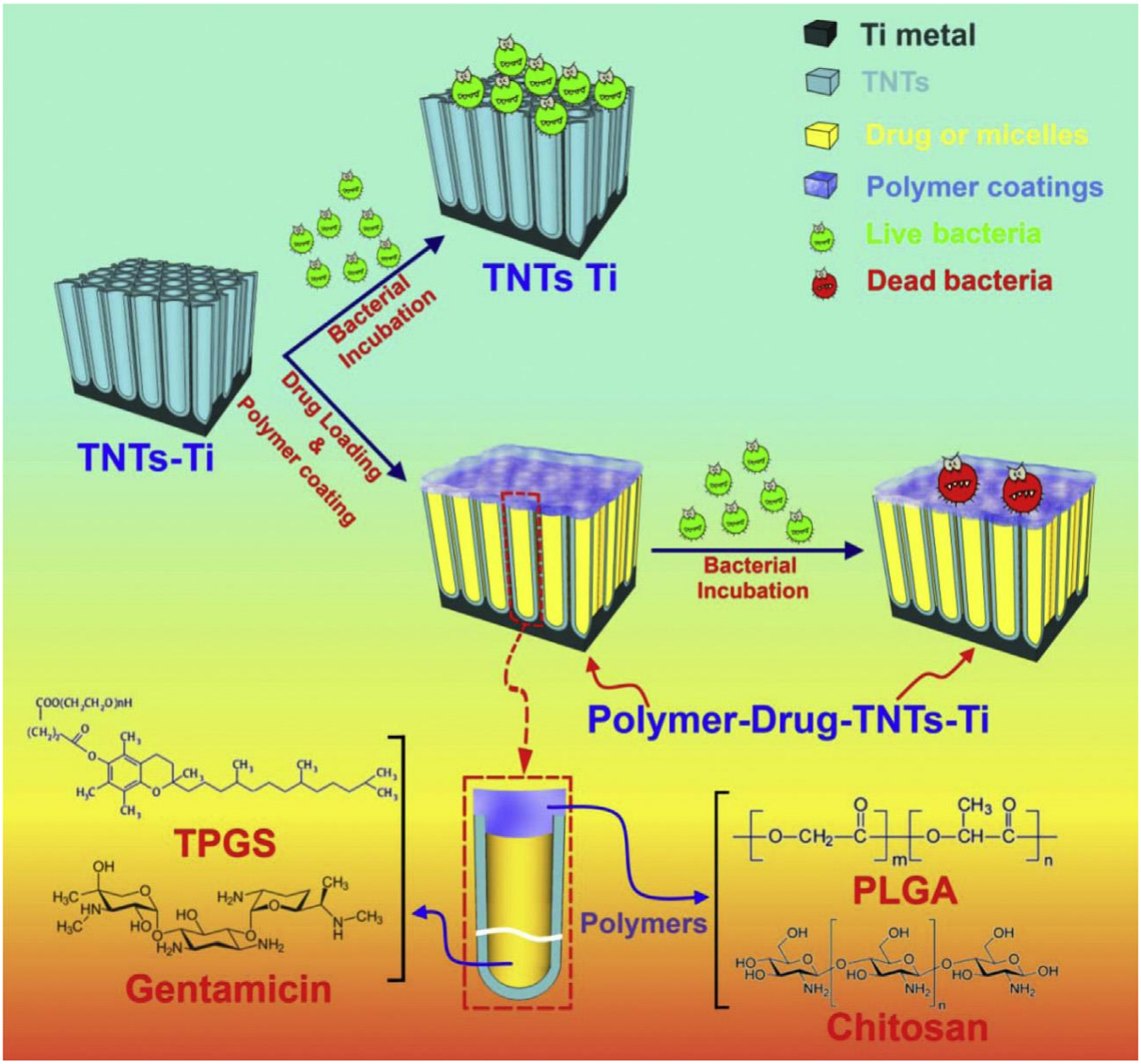

Figure 3: To control the release of gentamicin from TNTs and exert both cell adhesive and antibacterial activity, TNTs were first loaded with gentamicin (encapsulated in a micelle polymer nanocarrier, d-α-tocopheryl polyethylene glycol 1000 succinate, TPGS), and then covered by biopolymer coatings (polylactic-co-glycolic acid, PLGA, and chitosan). Reproduced with permission.[138] Copyright 2015, Elsevier.

Another approach, not sufficiently explored, would be the use of drug delivery systems, i.e. constructs already designed to encapsulate and release drugs in a controlled manner. Examples include micelles, liposomes and nanoparticles – which can moreover be functionalized with signaling molecules to improve receptor targeting. While drug delivery carriers functionalized with integrin-binding ligands (e.g. RGD peptides) have been widely used to target cancerous cells and specifically deliver cytotoxic (anti-cancer) drugs,[163] immobilization of these systems on biomaterials is not common.

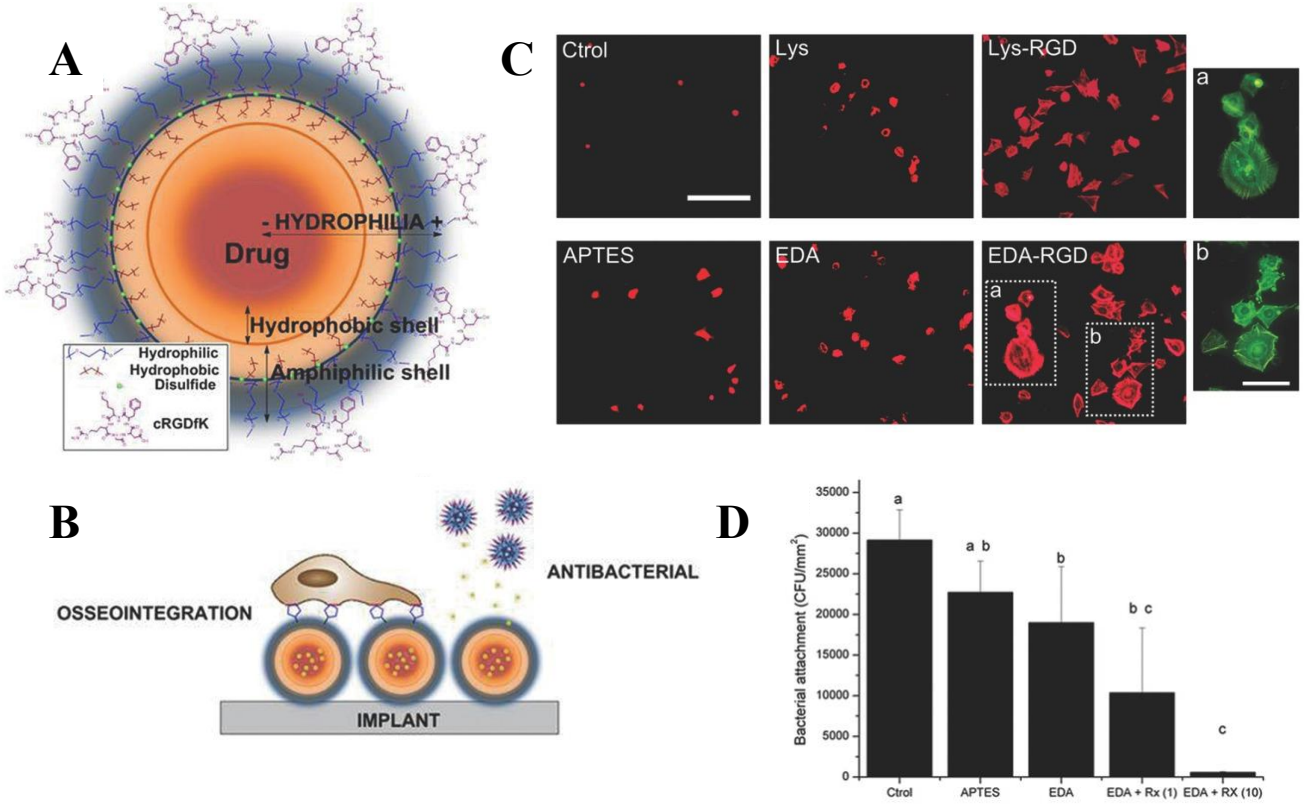

Figure 4: A) Schematic representation of the multifunctional nanoparticles (NPs). The combination of hydrophilic and hydrophobic moieties confers an amphipathic structure to the NP. The drug roxithromycin is encapsulated in the hydrophobic oily core of the NP and the surface is decorated with the cyclic RGD peptide c(RGDfK). B) Multifunctional activity of the NPs. C) Immunostaining of OB-like cells on Ti; the samples functionalized with RGD-decorated NPs promoted higher cell adhesion and focal adhesions than controls; D) Antibacterial effect of the coatings. Roxithromycin significantly inhibits *Streptococcus sanguinis* attachment in a concentration-dependent manner. Ctrol: Ti non-functionalized; APTES: Ti aminosilanized; Lys/EDA (ethylenediamine): Ti functionalized with NPs (different crosslinker used) without RGD; Lys/EDA-RGD: Ti functionalized with RGD-NPs. Reproduced (adapted) from [164].

In this regard, we recently described the use of RGD-decorated polyurethane-polyurea nanoparticles loaded with the antibiotic roxithromycin as multifunctional systems to functionalize Ti (Figure 4).[164] The multifunctional nanoparticles enhanced OB-like adhesion (cell numbers, spreading and focal adhesion formation) and proliferation compared to plain Ti and Ti functionalized with nanoparticles without the RGD motif. Simultaneously, the nanoparticles strongly suppressed the adhesion of *Streptococcus sanguinis* on the surfaces in a concentration (i.e. of roxithromycin)-dependent manner. The nanoparticles released 60-70% of the drug within the first 4-6 h, which would address the elevated risk of infection post-implantation,[165,166] but the remaining drug was released very slowly, allowing a sustained antibacterial effect at longer time periods. Interestingly, the remaining ca. 30% of drug was still efficient at inhibiting bacterial colonization at longer time points. Such design would thus tackle both acute infections post-surgery and chronic defense mechanisms; however, the application of this strategy on biomaterials remains to be fully explored.

Bovine serum albumin (BSA)-based nanoparticles (BNPs) are also gaining increasing attention as multifunctional systems with the capacity to control the release of diverse drugs. In a recent report, Lu and coworkers described nanostructured architectures on Ti surfaces by alternating layers of BNPs loaded with either BMP-2 or vancomycin.[167] The coatings were produced following a layer-by-layer approach, as BNPs were coated with chitosan or oxidized alginate to render positively or negatively charged BNPs, respectively. These coatings allowed a long-term sustained release of the drugs and showed a remarkable multifunctional potential: while the nanostructured texture and BMP-2 promoted BMSC adhesion, proliferation and osteogenic differentiation (i.e. increased ALP activity), vancomycin inhibited the growth of *Staphylococcus epidermidis* up to 7 days of incubation (Table 2).[167] These systems are versatile and can be used to encapsulate other substances. For example, in another study of the same group, BNPs-coated with chitosan and loaded with dexamethasone were combined with vancomycin-conjugated alginate to produce films with osteoinductive and antibacterial properties.[168]

3.3 Immobilization of peptides

The last multifunctional strategy focuses on the covalent immobilization of peptides. This approach, together with the use of nanostructured surfaces (see Section 5), is particularly attractive to combat infections, as it does not rely on transient drug-diffusion processes. Such processes are inherently limited and subjected to depletion over time, as well as having the risk of promoting antimicrobial resistance.

The co-immobilization of peptides has been widely explored to improve the osteoconductive and osteoinductive properties of biomaterials.[35] This strategy takes advantage of the well-defined structure, ease of synthesis and good stability of short peptides, but improves their often moderate to low bioactivity and specificity, better recapitulating the complex microenvironment of bone ECM. The combination of peptide motifs has proven useful to e.g. synergize the binding towards integrin α5β1 (RGD + PHSRN),[78,79,169] improve osteoblast functions via integrin and proteoglycan binding (RGD + KRSR/FHRRIKA)[80,170,171] or trigger integrin and growth factor signaling (RGD + BMP-derived peptides).[172,173] These approaches will not be covered here, but are described in detail in the literature.[35,174]

The combination of cell adhesive sequences with AMPs offers excellent opportunities to develop multifunctional biomaterials. It is important to note that AMPs display high potency against a broad spectrum of bacteria. Moreover, the mechanism of action of AMPs (i.e. interaction with bacterial membranes) appears to have a lower propensity to develop antibacterial resistance compared to

conventional antibiotics.[175,176,177,178] Following this rationale, the functionalization of Ti with an equimolar mixture of an RGD peptide and the AMP HHC36 inhibited the attachment of *Staphylococcus aureus* and *Escherichia coli* while improving bone marrow stromal cell (BMSC) adhesion.[179] Although the authors implemented a *click chemistry*-based methodology to modify the proportion of peptide grafting, controlling the concentration, ratio, and spatial organization of peptide mixtures upon binding to a surface is a challenging task and not always possible. To address that, we developed a peptidic branched platform with the capacity to simultaneously present two peptide sequences in a chemically controlled fashion.[78,79] Using this platform we recently combined the RGD sequence with LF1-11, an AMP derived from lactoferrin that showed excellent antibacterial properties on Ti surfaces.[180,181] Such approach very effectively improved OB adhesion, proliferation and mineralization, and inhibited *Staphylococcus aureus* and *Streptococcus sanguinis* attachment and biofilm progression (Figure 5).[182] Importantly, the bifunctional molecule was also effective in a co-culture scenario in which the surfaces were exposed to bacterial suspensions (pre-infective condition) for 2h before seeding OB-like cells. On non-functionalized surfaces the presence of bacteria drastically inhibited cell attachment. In contrast, on the surfaces coated with the RGD/LF1-11 platform, normal cell adhesion and viability was preserved. SEM analysis further revealed that in such a competitive scenario, bacteria directly interfered with OBs (e.g. by surrounding and covering them), preventing eukaryotic cells from attaching and adequately spreading. The multifunctional coating, through its dual cell adhesive and antibacterial effect, proved useful to overcome the deleterious effects of initial bacterial adherence. These data support the concept of the "race for the surface"[14,38] and indicates that rather than a competition cells actually "fight for the surface".

Although this strategy has potential to develop anti-infective coatings, it should be emphasized that surviving bacteria, even very low numbers, might be capable of proliferating on the implant surfaces, initiating the formation of new biofilms. Moreover, bacterial debris and proteins from the extracellular environment may serve as new anchoring points for other colonizers.[183] To solve this, cell adhesive and antibacterial peptides can be combined together with anti-adhesive polymer coatings to confer biomaterials with a trifunctional potential (cell adhesive, bacterial repellent/bacteriostatic and bactericidal). We recently followed this approach (Figure 6), combining PEG coatings electrodeposited onto Ti surfaces with the aforementioned RGD/LF1-11 platform, which was covalently attached to the PEG layers using a maleimide crosslinker.[184] As expected, PEG coatings inhibited protein adsorption and cell (both bacteria and OB-like cells) adhesion. However, the presence of the RGD sequence efficiently rescued cell adhesion, while the AMP increased the antibacterial potential of the coatings, reaching values of *Streptococcus sanguinis* adhesion below 0.2% (Table 2

and Figure 6). In another example, the triblock copolymer Pluronic F127 (PEG-polypropylene glycol-PEG) (PF127) was functionalized with either RGD or an AMP to coat the biomaterial surfaces.[185] In detail, surfaces were coated with different mixtures of PF127, PF127-RGD and PF127-AMP. By tuning the proportion of these polymers, antibacterial potential against *Staphylococcus aureus*, *Staphylococcus epidermidis*, and *Pseudomonas aeruginosa*, or improved FB adhesion could be obtained.

An alternative approach would be the combination of AMPs with GFs. In this regard, Yüksel et al. recently described a bilayer of PLGA membranes with antibacterial and bioactive properties.[186] The dual function was achieved by covalently immobilizing the AMP magainin II within one of the layers, and incorporating epidermal growth factor (EGF) in the other layer. This approach reduced the adhesion of *Escherichia coli* and *Staphylococcus aureus* and supported FB adhesion. This strategy opens the way to combine AMPs with other GFs (e.g. BMPs) or osteogenic peptides. Particularly interesting would be the co-immobilization of AMPs with BMP-derived peptides,[187,188] as this strategy would allow for an osteogenic effect at the implantation site, reducing the risk of an uncontrolled release of GFs. However, while RGD has been co-immobilized with peptides derived from BMP-2[172] or BMP-7,[173] showing enhanced osteogenic differentiation of stem cells, the combination of BMP-mimetics with AMPs remains to be explored. Another approach that deserves further investigation is to integrate dual functions within one single biomolecule. Bronk *et al*. engineered a collagen-mimetic molecule that upon immobilization on Ti enhanced OB-like cell adhesion and differentiation, and prevented *Staphylococcus aureus* and *Staphylococcus epidermidis* colonization.[189] Godoy-Gallardo *et al*. reported a simple but effective multifunctional strategy by grafting triethoxysilypropyl succinic anhydride (TESPSA) silane on Ti. Silanes have been widely used as crosslinker to attach bioactive peptide sequences; however, in this study, the silane alone enhanced the expression of osteogenic markers on OB-like cells, decreased the adhesion of *Streptococcus sanguinis* and *Lactobacillus salivarius*, and supported FB adhesion in a co-culture competitive setting in the presence of bacteria.[190] Yuran et al. recently reported a minimalistic bifunctional peptide combining the RGD sequence with two units of fluorinated phenylalanine (Phe(4-F)), which promoted peptide self-assembly into cell adhesive and bacterial resistant coatings.[191] The amino acid 3,4-dihydroxyphenylalanine (DOPA) was used as anchoring unit to bind the peptide to Ti surfaces (Table 2).

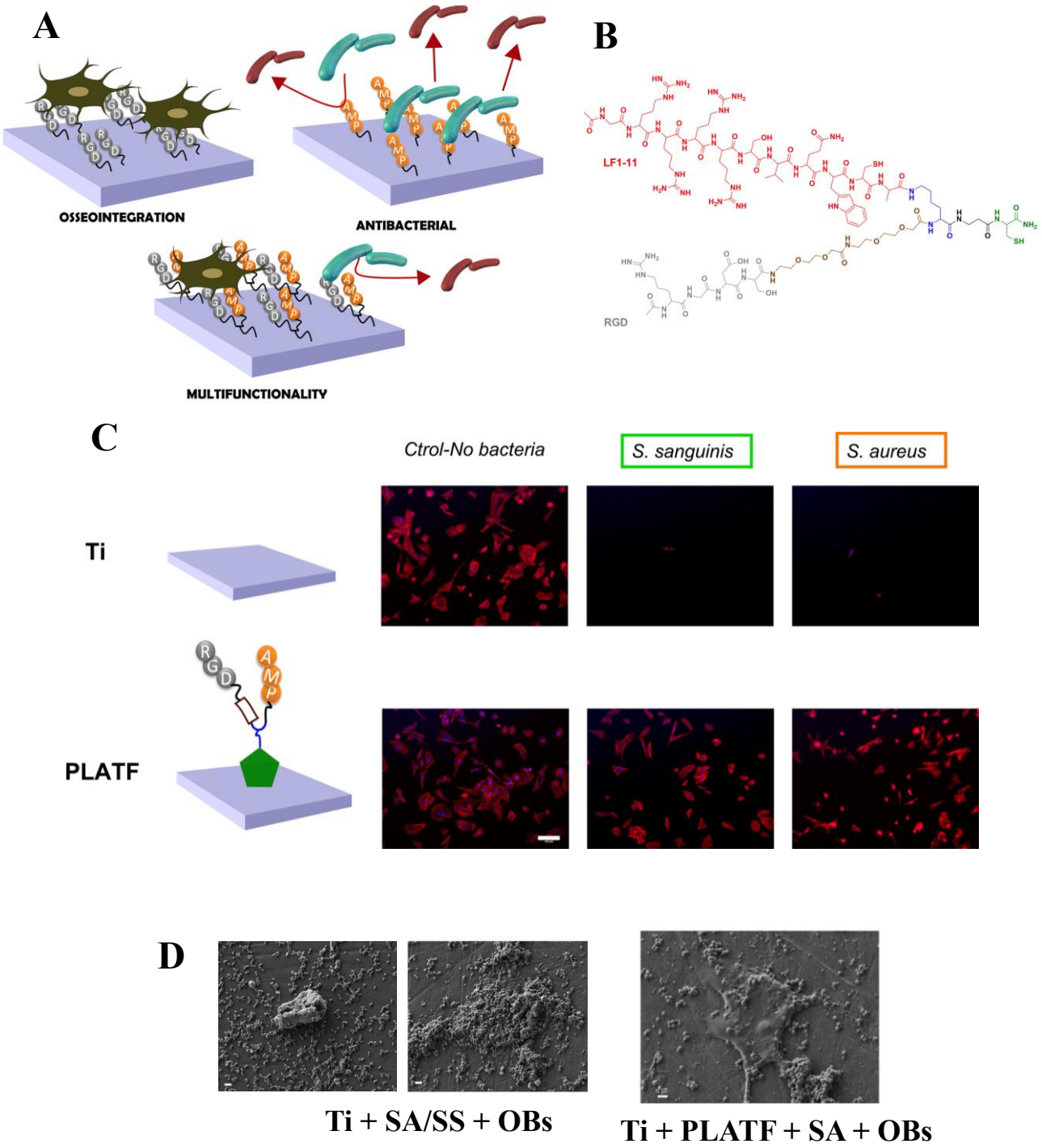

Figure 5: A) Classical approaches tend to functionalize surfaces with either cell adhesive or antibacterial peptides, but ignore a combined effect. Using a peptidic platform both activities can be simultaneously exploited on the biomaterial surface; B) Chemical structure of the multifunctional platform; C) Immunostaining of actin fibers on cell-bacteria co-culture studies. Pre-incubation of Ti surfaces with bacteria (*S. sanguinis* or *S. aureus*) inhibits the adhesion of OB-like cells (upper row); functionalizing the surfaces with the platform restores cell adhesion to normal levels (lower row); D) SEM analysis of OB-bacteria interactions. In the absence of the platform bacteria surround cells and block their spreading. SS: *S. sanguinis*; SA: *S. aureus*. Reproduced (adapted) with permission.[182] Copyright 2017, American Chemical Society.

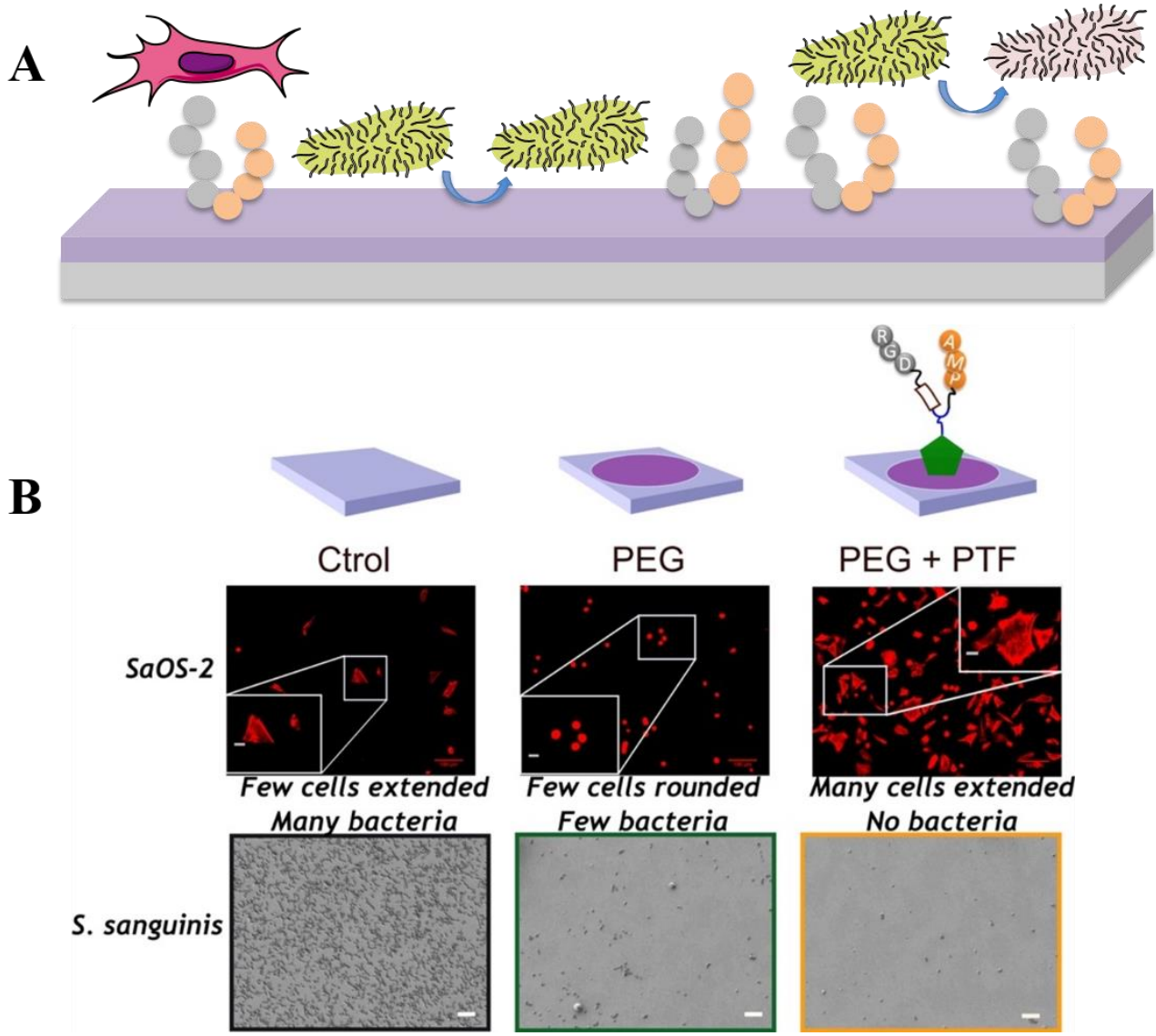

Figure 6: A) Trifunctional strategy: i) a repellent coating (e.g. PEG) prevents bacterial attachment; ii) a cell adhesive sequence (e.g. RGD) supports eukaryotic cell adhesion; and iii) a bactericidal molecule (e.g. AMP) kills adhering bacteria; B) Combining the low fouling potential of PEG with a cell adhesive/bactericidal platform (RGD + LF1-11) efficiently supports OB-like cell adhesion but totally suppresses the adhesion of *S. sanguinis*. Figure 6B is reproduced with permission.[184] Copyright 2018, Elsevier.

Table 1. Selection of representative examples of multifunctional approaches on biomaterials

Strategy	Biofunctional elements	Substrate + coatings (immobilization method)[a]	Main biological effects[b]	References
Functionalized anti-adhesive polymer	PEG + RGD	Ti + PLL-g-PEG (electrostatic adsorption) + RGD (vinyl sulfone-thiol)	↓ *S. aureus* adhesion; Cell adhesion not studied	[106]
	PEG + RGD	Ti + PLL-g-PEG (electrostatic adsorption) + RGD (vinyl sulfone-thiol)	↓Bacterial adhesion (several strains); Cell adhesion not studied	[107]
	PEG + RGD	Ti + PLL-g-PEG (electrostatic adsorption) + RGD (vinyl sulfone-thiol)	↓ *S. epidermidis* adhesion; ↑ OB-like adhesion	[108]
	PEG + RGD	Ti + PEG (several methods) + RGD (physisorption)	↓ *S. sanguinis* and *L. salivarius* adhesion; ↑ FB adhesion	[109]
	Dextran + BMP-2	Ti6Al4V-dopamine + dextran (reductive amination) + BMP-2 (reductive amination)	↓ *S. aureus* and *S. epidermidis*; ↑ OB response	[110]
	PMAA + silk sericin	Ti + PMAA (silanization + SI-ATRP) + silk sericin (carbodiimide chemistry)	↓ *S. aureus* and *S. epidermidis* adhesion; ↑ OB response	[111]
	HA + VEGF	Ti + catechol-HA (direct chemisorption) + VEGF (carbodiimide chemistry)	↓ *S. aureus* adhesion; ↑ OB response	[112]
Functionalized bactericidal polymer	CM-CH + VEGF	Ti-dopamine + CM-CH (carbodiimide chemistry) + VEGF (carbodiimide chemistry)	↓ *S. aureus* adhesion; ↑ OB response	[112]
	HA/CH + RGD	Ti + HA/CH (PEMs electrostatic adsorption) + RGD (carbodiimide chemistry)	↓ *S. aureus* adhesion; ↑ OB response	[121]
	CH + RGD	Ti-dopamine + CH (glutaraldehyde crosslinking) + RGD (carbodiimide chemistry)	↓ *S. aureus* and *S. epidermidis* adhesion; ↑ OB response	[122]
	CM-CH + BMP-2	Ti6Al4V-dopamine + CM-CH (carbodiimide chemistry) + BMP-2 (carbodiimide chemistry)	↓ *S. aureus* and *S. epidermidis* adhesion; ↑ OB and MSC response	[123]
	CM-CH + ALP	Ti-dopamine + CM-CH (carbodiimide chemistry) + ALP (carbodiimide chemistry)	↓ *S. epidermidis* adhesion; ↑ OB, MSC and ADSC osteogenic differentiation	[125]
	CH/PAA + Ga	Ti + PAA (electropolymerization) + CH-Ga (electrochemical deposition)	↓ *E. coli* and *S. epidermidis* viability; OB-like adhesion supported and ↑ BMP-2 expression	[126]

Osteoconductive /osteoinductive surface loaded w/ antibacterial agents	TNT + Ag	Ti > TNT (anodization) + Ag (electrodeposition)	↓ *P. aeruginosa* adhesion; Biocompatible for OBs	[132]
	TNT + Ag_2O NPs	Ti > TNT-Ag_2O (TiAg magnetron sputtering and anodization)	↓ *S. aureus* and *E. coli*; OB-like response not influenced compared to TNTs	[133]
	TNT + Zn	Ti > TNT (anodization) + Zn (hydrothermal treatment)	↓ *S. aureus* adhesion and proliferation; ↑ OB-like response; ↑ Bone formation *in vivo*	[135]
	TNT + gentamicin + CH/PLGA	Ti > TNT (anodization) + gentamicin (drop casting) + CH/PLGA (dip coating)	↓ *S. epidermis* viability; ↑ OB-like response	[138]
	HAp + Ag_2O + SrO	Ti + HAp/Ag_2O/SrO (plasma spray)	↓ *P. aeruginosa* viability; ↑ OB-like response for HAp + Ag/Sr compared to HAp	[150]
	CaP + HHC36	Ti + HAp (electrolyte deposition) + HHC36 (physical adsorption)	↓ *P. aeruginosa* and *S. aureus* viability; ↑ OB-like cell adhesion; ↑ Bone formation *in vivo*	[154]
	cRGD + roxithromycin	Ti + RGD-NPs/roxithromycin (silanization; roxithromycin is loaded by emulsification)	↓ *S. sanguinis* adhesion; ↑ OB-like response	[164]
	BMP-2 + vancomycin	Ti + BNP/BMP-2 + BNP/vancomycin (layer-by-layer adsorption; drugs are loaded by a desolvation method	↓ *S. epidermidis* growth; ↑ BMSC response	[167]
Immobilized peptides	RGD + HHC36	Ti + RGD/HHC36 (silanization + click chemistry)	↓ *S. aureus* and *E. coli* adhesion; ↑ BMSC adhesion	[179]
	RGD + LF1-11	Ti + RGD/LF1-11 (silanization)	↓ *S. aureus* and *S. sanguinis*; ↑ OB-like response	[182]
	PEG + RGD + LF1-11	Ti + PEG (electrodeposition) + RGD/LF1-11 (maleimide-thiol chemistry)	↓ *S. sanguinis*; ↑ OB-like response	[184]
	PF127 + RGD + AMP	Silicon + PF127/PF127-RGD/PF127-AMP (physical adsorption)	↓ *S. aureus*, *S. epidermidis* and *P. aeruginosa* adhesion; ↑ FB adhesion	[185]
	EGF + magainin II	PLGA + EGF (physical entrapment) + magainin II (carbodiimide chemistry)	↓ *S. aureus* and *E. coli* adhesion; ↑ FB adhesion	[186]
	Collagen-mimetic	Ti + collagen-mimetic (physisorption)	↓ *S. aureus* and *S. epidermidis* adhesion; ↑ OB-like adhesion and differentiation	[189]
	TESPSA silane	Ti + TESPSA (silanization)	↓ *S. sanguinis* and *L. salivarius* adhesion; ↑ OB-like differentiation; ↑ FB adhesion	[190]
	RGD + Phe(4-F)	Ti + DOPA-peptide (chemisorption)	↓ *E. coli* adhesion; ↑ OB-like adhesion	[191]

[a] “Substrate” refers to the material used, and “coating” to the combination of chemical entities that exhibit multiple biological activity; the methods used to immobilize the coatings are described in brackets.

[b] Only the main biological effects are highlighted. Reduced bacterial adhesion commonly indicates a reduction in bacterial cell numbers compared to controls. Improved cell response usually refers to increased values of cell adhesion, proliferation and differentiation compared to controls. Detailed data can be found in the corresponding references.

Abbreviations used: ADSC = adipose-derived stem cell; BMSC = bone marrow stromal cell; BMP = bone morphogenetic protein; BNP = BSA-based nanoparticle; CH = chitosan; CM-CH = carboxymethyl chitosan; cRGD = cyclic RGD; DOPA = 3,4-dihydroxyphenylalanine; FB = fibroblast; HA = hyaluronic acid; HHC36 peptide = (KRWWKWWRR); MSC = mesenchymal stem cell; NP = nanoparticle; OB = osteoblast; PAA = poly(acrylic acid); PEG = poly(ethylene glycol); PEMs = polyelectrolyte multilayers; Phe(4-F) = fluorinated phenylalanine; PLL-g-PEG = poly-L-lysine-graft-poly(ethylene glycol); PMAA = poly(methacrylic acid); SI-ATRP = surface initiated atom transfer radical polymerization; VEGF = vascular endothelial growth factor;

Bacterial strains: *Escherichia coli = E. coli; Lactobacillus salivarius = L. salivarius; Pseudomonas aeruginosa = P. aeruginosa*; *Staphylococcus aureus = S. aureus*; *Staphylococcus epidermidis = S. epidermidis*; *Streptococcus sanguinis = S. sanguinis*; *Streptococcus mutans = S. mutans*.

4. Osteogenic nanotopographies

We have already discussed that implant osteointegration can be enhanced by physical and chemical methods. While physical modifications (i.e. surface roughness) improve implant functionality by increasing its micromechanical retention with bone, chemical coatings such as integrin-binding molecules or CaP have been described to promote osteogenesis from mesenchymal stem cells (MSCs). While roughness is undoubtedly useful, it is hard to dissect effects as surfaces with two similar Ra values can appear very different and so could potentially have different effects on cells. This section of the review will focus on cell response to defined nanotopography with particular consideration on nanotopographically-directed osteogenesis. We note that roughness based approaches are being developed – most notably for orthopedic application (see Section 2.1). These are not a focus of this review, but excellent reviews are available.[192,193]

The ability of surface topography to guide cells has been known for over 100 years,[194] with the term 'contact guidance' becoming used in the 1950/60s.[195,196]. In the 1980s, understanding of the cell-topographical interaction at the microscale started to become elucidated thanks to microfabrication techniques such as photolithography and wet/dry etch.[197,198] This proliferation of biological data revealed that all cell types tested responded to microtopographical features.[199,200,201,202,203,204,205] As semiconductor technology advanced to help develop faster computer microchips, the study of nanotopographical-cell interactions became possible with first indications of the cells' ability to contact guide to nanopatterns shown using substrates derived from laser holographical lithography.[206] By the turn of the 21st century, both top-down (lithographical, e.g. electron beam lithography, colloidal lithography[207,208,209]) and bottom up (e.g. polymer phase separation, block co-polymer separation, etc.[210,211,212,213]) approaches were becoming available to cell biologists. These substrates allowed development of understanding that cells could respond to features where all features were nanoscale;[214] soon it was understood that a broad range of cells could respond to nanoscale features[215] – even platelets.[216]

Considering controlled topography, top-down techniques such as electron beam lithography (EBL) allow patterning for cell experimentation with features down to 10 nm in size.[217] Moving from cell-scale to clinical-scale may, however, be challenging for such techniques.

In contrast, bottom-up techniques such as polymer phase separation,[211] colloidal lithography,[218] block co-polymer lithography[219] and micelle lithography[220] where larger areas can be fabricated more simply – but with some loss of the resolution that EBL can offer

– are gaining popularity. However, for bone formation perhaps this is not so important. A study using EBL to fabricate nanopits with 120 nm diameter, 100 nm depth and 300 nm-center-to-center positioning in a square pattern showed that MSCs did not form osteoblasts when the features were precisely placed (in fact a later study showed enhanced MSC self-renewal[221]) – rather osteoblast specific differentiation was only observed when the features were slightly offset (by up to ± 50 nm from the center positioning) (Figure 7A).[222] It is thus noteworthy that block co-polymer micelles can now be fabricated almost to the scale that EBL has been used to generate controlled nanodisorder, i.e. with ± 50 nm feature offsets known to drive cell function.[223] Copies (via nickel shims) of phase separated nanosurfaces and colloidal nanosurfaces in bio-polymers (polymethylmethacrylate and polycaprolactone) have now been shown to influence MSC growth *in vitro*.[224] Further, such bottom-up methodologies have been used to generate masks for anodization of e.g. Ti implant materials to enhance osteogenesis.[225,226,227,228]

Moving into 3D is challenging for lithographical and demixing processes due to their 2D natures. Interestingly for tissue engineering, polymer demixing can be performed inside 3D constructs such as tubes[229] and, indeed, influence MSC growth.[230] Tube-like structures are typical in bone e.g. Haversian and Volkman's canals (the osteon system). A further major development towards 3D is a topographical approach with the potential to incorporate ultra-precise (e.g. lithographical) nanotopographical fabrication.[231] In this system, a biodegradable polymer (e.g. polycaprolactone) was embossed between two micron or nanopatterned surfaces. Included in the design were spacing posts (approx. 50 μm high) to allow perfusion of media and oxygen during pre-conditioning. The embossed sheet was rolled to form a larger construct and seeded with cells prior to pre-conditioning *in vitro*. Also, 'car-park' assemblies have been made using osteogenic micropatterns embossed onto polymeric sheets that incorporate large spacers to separate layers of the 'car-park';[232] embossing of osteogenic nanotopographies in this system is easily envisaged.

If we consider mechanism of cellular response, cell adhesions are very sensitive to nanoscale features, being able to form filopodia in response to topographies down to 10 nm in height[233] but, further, being seen to have to have 'nanopodial' interactions down to 8 nm in height.[234] At the microscale, contact guidance by features of similar scale to the cells themselves is easy to envisage (i.e. they have no choice). At the nanoscale, however, subcellular features, i.e. adhesions, must reorganize to guide cells. As adhesive proteins encounter a nanoscale cue (e.g. a nanogroove or a fibronectin line) - an order of magnitude smaller than the cell, but on a similar

scale to filopodia and integrin receptors - the adhesions will elongate along the cue and this, in turn, will drive actin alignment in the direction of the cues.[235] This will align the cell literally, and metaphorically, from the bottom-up (in fact, this is a first step for large scale tissue organization during development).

In the context of this review, particularly studied has been MSC to osteoblast (bone forming progeny) differentiation. A range of nanoscale topographies from nanodisordered surfaces,[222] to biomimetic helical structures with collagen-like 63 nm periodicity[236] has been demonstrated to induce osteogenesis (Figure 7B).

At the cell-material interface, cell adhesion formation has been widely studied and is considered important in defining MSC to osteoblast differentiation. When observing MSC differentiation to bone, it is not the number of adhesions that a cell can form *per se* that is important for bone production, rather the size of the adhesions. Studying MSC adhesion size during osteogenesis shows that larger adhesions form.[222] In addition, it has been shown using RGD functionalized gold nanopatterns that a slight disorder significantly enhances MSC adhesion.[220] It has been seen that disorder can increase adhesion through bringing groups of adhesive points closer together, into a critical 70 nm range[237] to facilitate gathering of integrins into focal adhesions and thus facilitate integrin gathering. Also, MSCs cultured on osteogenic nanopatterns have been indicated to express endogenous vitronectin over fibronectin.[238] Vitronectin may be important, as it allows better bridging between integrin clusters via intracellular adhesion proteins such as vinculin and talin.[239] Efficient bridging will allow cells to form larger, more mature adhesions, over discontinuities such as nanopits.

In further consideration of adhesion mechanism, the formation of “super-mature” adhesions (SMAs)[240] (> 5 μm long) is important for stabilizing the large osteoblast morphology and resultant bone formation. It is likely that such super-mature adhesions are stabilized/scaffolded by proteins such as RACK1,[241,242] allowing increased levels of intracellular tension,[243,244] mediated by RhoA Kinase (ROCK), important to MSC fate.[245,246,247]

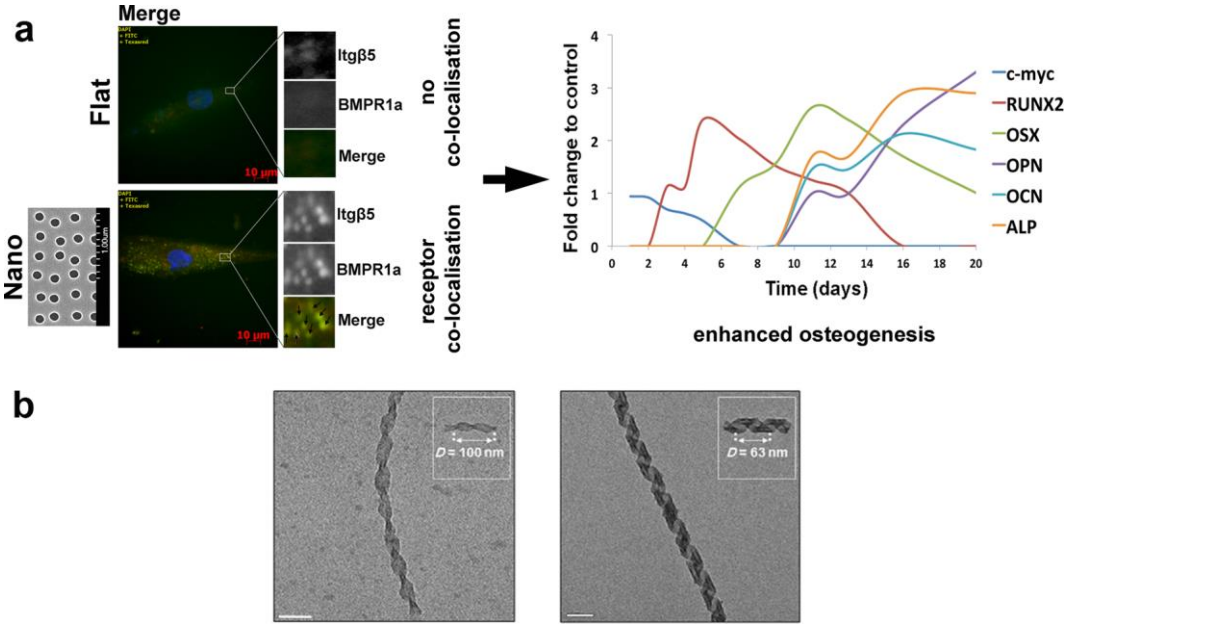

Figure 7. Nanoscale topographical control of MSC differentiation. (A) MSCs respond to nanoscale disorder. Using electron beam lithography to fabricate arrays of nanopits (120 nm diameter, 100 nm deep) in a square array (SQ, 300 nm center-center pitch) with up to ± 50 nm offset from the center square position (nano), increased adhesion and adhesion co-localization of integrin (here integrin beta 5 is stained) and the BMP2 receptor (here BMPR1a is stained) and this drives MSC osteogenic progression, as demonstrated by expression patterns of the osteogenic genes RUNX2 (runt related transcription factor 2), osterix (OSX), osteopontin (OPN), osteocalcin (OCN) and alkaline phosphatase (ALP). Reproduced (adapted) under the terms of the Creative Commons Attribution 4.0 International license (CC BY 4.0) [238] Copyright 2014, American Chemical Society. (B) Synthetic collagen banding patterns with 100 nm repeat (non-physiological) and 63 nm repeat (physiological); MSCs are stimulated to undergo osteogenesis on the physiological pattern, but not the non-physiological pattern. Reproduced (adapted) with permission.[236] Copyright 2013, American Chemical Society.

5. Antimicrobial nanotopographies

We have seen in the previous sections that current strategies to combat biomaterials-associated infections are largely reliant upon chemical means i.e. use of polymers (or surface functional groups) to prevent protein adsorption and inhibit bacterial adhesion, or coatings that release chemical agents such as antibiotics, silver ions or quaternary ammonium salts into the surrounding microenvironment. A critical limitation of these chemistry-based strategies is that they are transient because leaching of antimicrobial agents is limited and subject to depletion over time. Dwindling antibiotic concentration and/or prolonged bacterial colonization of materials may also inadvertently promote development and spread of antimicrobial resistance. A physical approach, such as topography, could potentially overcome the above problems and offers completely new and alternative solutions to biomaterial infections.

5.1 Anti-biofouling nanotopographies

Surface topography has been known to alter bacterial adhesion and biofilm formation. It has become evident that surface hydrophobicity/hydrophilicity and effective contact area are two key factors that are responsible for the different bacterial adhesive behavior on surfaces. A well-known example is the superhydrophobic 'lotus effect', which is the result of a combination of hydrophobic chemistry (wax) and the hierarchical and multiscale surface structure, i.e., nanostructures on microstructures. The hydrophobic epicuticle layer, with high density of nano-featured wax crystalloids, covers micro-featured convex surface structures, creating a surface with very high contact angle (ca. 161°).[248] It was found that when the surface of a lotus leaf was dipped in ethanol to remove the wax, the contact angle of a water drop decreased dramatically from ca. 161° to 122°, and the water droplet was pinned to the surface.[249] This intrinsic hydrophobicity of the surface principally originated from the pure hierarchy of multiscale structures, similar to that observed on the surface of a rose petal. The lotus effect requires air to become "trapped" between the nanostructures on the surface, i.e. the Cassie and Baxter state, while the rose petal effect allows the liquid film to impregnate the micro/nano topographies, i.e. the Wenzel state, because the non-waxy petal surface has a good wetting characteristics with water. Many plant leave surfaces with micro/nano-topographies, e.g. rice and taro, have been shown to be able to control the bacterial fouling and biofilm formation.[250,251] Inspired by nature, various nanoengineered surfaces have been investigated in terms of their surface hydrophobicity/hydrophilicity and nanotopography. Hizal et al.[252] reported two nanostructured superhydrophobic surfaces with extremely low bacterial adhesion under dynamic flow condition. Both 2D nanoporous surface and 3D nanopillared surface showed a significant reduction in adhesion for *Staphylococcus aureus* and *Escherichia coli*, which was more pronounced for the hydrophobic surface treated with a Teflon coating (Figure 8). This was attributed to a decreased contact area for the 2D porous surface and effective air entrapment in 3D nanopillars. The bacterial adhesion force on these nanoengineered surfaces was reduced as measured by atomic force microscopy (AFM). Similar anti-fouling effects were observed on hydrophilic TiO_2 nanopillars[253] or nanotubes.[254] The nanofeature dimensions e.g. nanopillar diameter, height and spacing affected the bacterial adhesion due to the change of effective contact area.[255,256] Strong bacterial repelling has also been reported on highly ordered alumina nanoporous surfaces[257] and polymer (PLGA) nanopit surfaces with pore sizes ranging from 200 to 500 nm.[258] This contact-area-reducing approach has been attempted in real medical applications. Serrano et al.[259] reported oxygen plasma treated sutures with lamellae voids with feature size ≤ bacteria size. The results showed that bacterial attachment was

decreased with reduced surface contact area and effective prevention of biofilm formation was achieved in absorbable sutures with top area fractions below 30% presenting lamellae with 200-500 nm thickness and several microns in length, separated by 1-2 um voids.

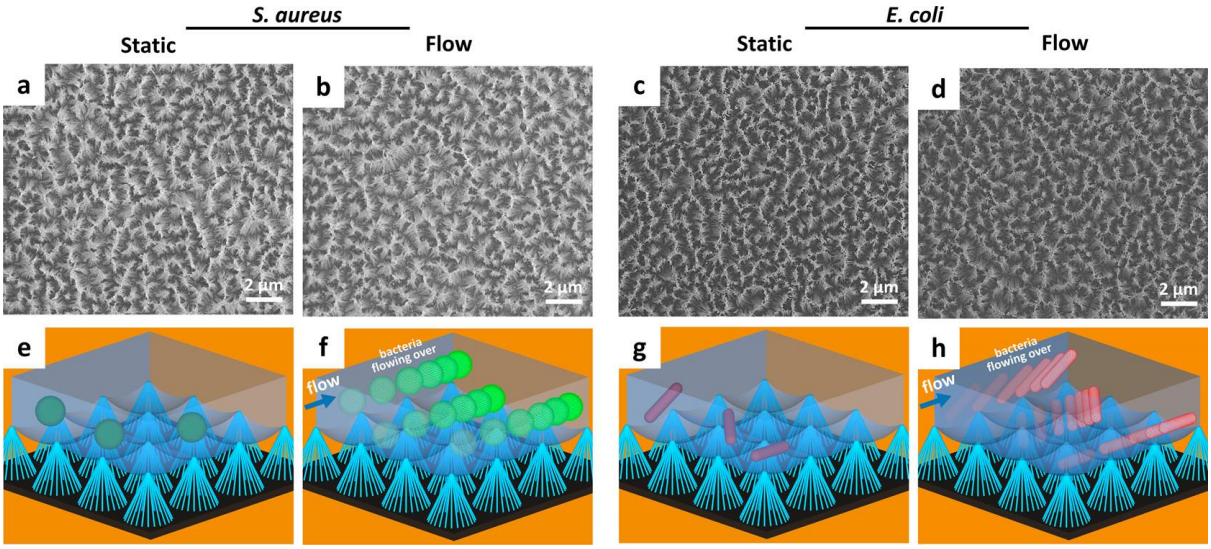

Figure 8. FE-SEM images (a–d) and schematics (e–h) representing the bacterial adhesion on hydrophobic nanopillared surfaces. In panels e and g, the schematics represent the bacteria are floating over the entrapped air layer under static conditions. In panels f and h, the schematics represent the bacteria being washed off under flow. Reproduced with permission.[252] Copyright 2017, American Chemical Society.

5.2 Bactericidal nanotopographies

Bactericidal nanotopographies have not been reported until recently, although bactericidal nanostructures in the form of suspended colloids were investigated much earlier. For example, Liu et al. reported that the single-walled carbon nanotubes (SWCNTs) in a suspension are bactericidal upon contact with bacteria. They found that the sharpness and concentration of the SWCNTs coupled to mechanical shaking of the SWCNT suspension could enhance the bacteria-killing performance. They described these SWCNTS as ‘nano darts’ which were able to physically pierce the bacterial cells.[260]

Ivanova et al. first reported bactericidal nanotopographies on cicada (Psaltoda claripennis) wings. When culturing *Pseudomonas aeruginosa* cells on Psaltoda claripennis wings, which comprised 200 nm tall nanopillars (or nanocones) with a diameter of 100 nm at the base and 60 nm at the cap, and spaced 170 nm apart from center to center, it was noted that the bacterium died.[261] They postulated that cell death was caused purely by the mechanical rupturing of bacterial cell walls. A biophysical model has been developed to explain the mechano-

bactericidal action of the cicada wings.[262] Kelleher *et al*. tested three different cicada wings (Megapomponia intermedia, Ayuthia spectabile and Cryptotympana aguila).[263] They found a strong correlation between the bactericidal properties of the wings and the scale of the nanotopographies present on the different wing surfaces. Sharper and more densely packed nanopillars on Megapomponia intermedia wings killed more bacteria, probably by inducing a greater strain on the bacterial cell walls. Subsequently, more naturally occurring bactericidal surfaces have been reported.[264,265] They include nanopillars on the dragonfly wing,[266] the damselfly wing,[267] the moth eye,[268] the rat-tailed maggot, the aquatic larva of the Drone fly,[269] and the nanotipped hairs on gecko skin.[270]

Inspired by nature, a number of studies have since been carried out to develop bactericidal nanotopographies on synthetic materials. They include silicon[271,272,273,274] and diamond coated silicon,[275,276,277] titanium and its alloy,[278,279,280,281,282,283,284] polymers,[285,286,287,288] stainless steel[289] and aluminium.[290] Table 3 lists a summary of biomimetic bactericidal surfaces on various materials currently in development. Examples of some bactericidal nanotopographies created on various synthetic materials are shown in Figure 9.

Table 3. Current development in biomimetic and bio-inspired bactericidal surfaces on various substrates.

Material	Surface nanotopography	Fabrication method	Bacteria studied	Ref
Silicon	Nanopillars Nanoneedles Nanowires	Reactive ion etching (RIE), metal-assisted chemical etching	*Pseudomonas aeruginosa, Staphylococcus aureus* and *Bacillus subtilis*	[271,272,273, 274]
Diamond and diamond coated Si	Nanocones	Chemical vapour deposition (CVD) + bias assisted RIE	*Pseudomonas aeruginosa*	[275]
	Nanoneedles	RIE + CVD	*Pseudomonas aeruginosa, Escherichia coli,* and *Streptococcus gordonii*	[276,277]
Titanium	Nanowires	Hydrothermal growth	*Staphylococcus aureus, Staphylococcus epidermidis, Pseudomonas aeruginosa, Escherichia coli, Bacillus subtilis, Enterococcus faecalis* and *Klebsiella pneumoniae*	[278,279,280, 281]
	Nanocolumns	Glancing angle sputter deposition	*Escherichia coli* and *Staphylococcus aureus*	[282]
	Nanopillars	Reactive ion etching	*Escherichia coli, Pseudomonas aeruginosa, Staphylococcus aureus* and *Mycobacterium smegmatis*	[283]
Ti alloy	Nanocones Nanowire	Thermal oxidation	*Escherichia coli*	[284]
Polymers	Nanopillars Nanocones	Nanoimprinting	*Escherichia coli, Pseudomona aeruginosa* and *Staphylococcus Aureus*	[285,286,287]
	Nanopillars Nanocones	Colloidal lithography	*Escherichia coli* and *Klebsiella pneumoniae*	[288]
Stainless steel	Nano-protruding textures	Electrochemical etching	*Escherichia coli* and *Staphylococcus aureus*	[289]
Aluminium	Micro/nano-rough surfaces	Chemical etching	*Escherichia coli, Klebsiella pneumoniae* and *Staphylococcus aureus*	[290]

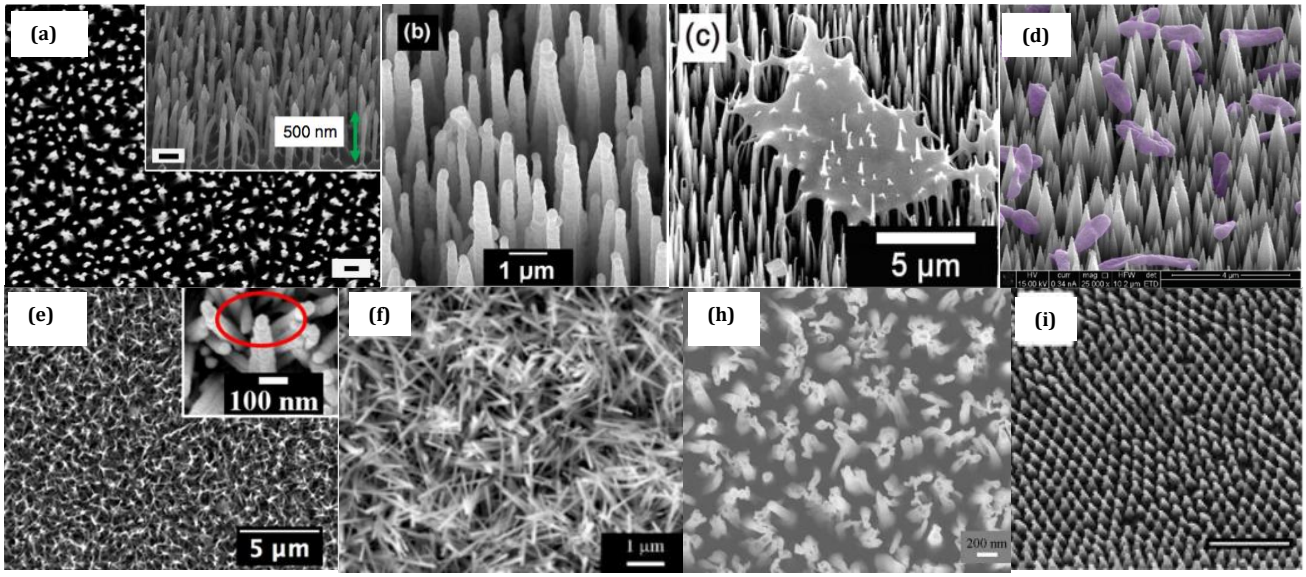

Figure 9. Examples of various synthetic bactericidal nanotopographies on different substrates.

(a) Black silicon (bSi). Reproduced with permission.[271] Copyright 2013, Springer Nature; (b) Diamond coated bSi. Reproduced with permission.[276] Copyright 2016, The Royal Society of Chemistry; (c) A pierced bacterium on bSi. Reproduced with permission.[277] Copyright 2018, The Royal Society of Chemistry; (d) Diamond nanocones. Reproduced with permission.[275] Copyright 2016, American Vacuum Society; (e) Hydrothermal TiO_2 nanowires.[278,280] Reproduced under the terms of the Creative Commons Attribution 4.0 International license (CC BY 4.0).[280] Copyright 2018, Springer Nature; (f) TiO_2 nanowires by thermal oxidation. Reproduced with permission.[284] Copyright 2016, Elsevier; (h) Black titanium (bTi). Reproduced under the terms of the Creative Commons Attribution 4.0 International license (CC BY 4.0).[283] Copyright 2017, Springer Nature; (i) PMMA nanocones. Reproduced with permission.[285] Copyright 2015, American Vacuum Society.

Ivanova *et al*. first reported the studies of biomimetic bactericidal surfaces on synthetic materials in 2013,[271] shortly after their discovery of bactericidal cicada wings in 2012.[261] Nanoprotruding surfaces with high-aspect-ratio nanopillars with a diameter of 20-80 nm and a height of 500 nm were generated on silicon substrates using a reactive ion etching (RIE) method, creating 'black silicon' (bSi), which mimics the wings of the dragonfly Diplacodes bipunctata. Notably, the bSi surfaces exhibited bactericidal activity towards both Gram-positive and Gram-negative bacteria. Notably, the range and bactericidal efficacy were larger than their biological analogues (cicada and dragonfly wings). Further study indicated that the bactericidal efficacy was strongly dependent on their feature sizes. Smaller and more densely packed pillars exhibited the greatest bactericidal activity.[273] The decrease in the nanopillar heights, nanopillar cap diameter and inter-nanopillar spacing corresponded to a subsequent decrease in the number of attached cells for both Gram-positive and -negative bacterial species.[273]

Similar nanopillar and nanowire surfaces using different etching methods also displayed similar bactericidal activity.[272,273,274] Susarrey-Arce *et al*. investigated the interaction and the viability

of bacteria of highly-oriented silicon nanowires (SiNWs) with and without functionalization. They found that the bare SiNWs and SiNWs functionalized with a silane (APTES) exhibited some degree of intrinsic bactericidal activity towards *Escherichia coli* and *Staphylococcus aureus*. However, bacterial cells could still proliferate for a long time on these topographic surfaces. By functionalization with chlorhexidine digluconate (CHD), the antimicrobial performance was greatly enhanced because CHD released from the surface had the potential to decrease the viability of both sessile and planktonic bacterial cells. They have also identified two different growth modes producing distinct in-plane and out-of-plane bacterial colonies for *Escherichia coli* and *Staphylococcus aureus*, respectively.[274] However, silicon is a non-load-bearing material and thus has limited application in biomedical implants.

Diamond coating using thin film technology is becoming an attractive approach for material functionalization for biomedical applications due to its unique properties. It is bioinert and its electrical conductivity can be tuned from insulating to near-metallic, which makes it a potential candidate material for orthopedic and neural device applications.[291] Fisher *et al.* demonstrated that diamond nanocone arrays deposited on a silicon substrate via microwave plasma CVD followed by bias-assisted RIE were bactericidal towards *Pseudomonas aeruginosa*.[275] Similar antimicrobial performance has also been reported for diamond coated bSi nanoneedles.[276,277] Interestingly, such a diamond coating or film could be deposited on Ti substrates, which may have important medical implications, as Ti metal and its alloys are widely used materials in orthopedic, dental and cardiovascular applications.

Because of the wide applications of Ti in biomedicine and the frequent biomaterials associated infections, the generation of antimicrobial nanosurfaces directly on Ti substrates would be desirable. Inspired by the cicada wings, Diu *et al*. first investigated bactericidal property and biocompatibility of nanowires grown directly on Ti substrates using an alkaline hydrothermal method.[278] It was found that motile and Gram-negative bacteria are more susceptible to killing than non-motile and Gram-positive ones. Culturing in dynamic (shaking) conditions also induced more killing compared to standard static bacterial cell culture condition. It is suggested that the thicker cell wall (peptidoglycan layer) found in Gram-positive cells and a lack of motility in non-motile cells may be responsible for their inferior susceptibility to killing.

Similar works have reported on hydrothermal nanowires with various bactericidal performances depending on processing and culturing conditions.[279,280,281] Cao *et al.* investigated longer-term biofilm formation of *Staphylococcus epidermidis* on spear or brush-type and pocket or niche-type nanowires. Pocket-type nanowire surfaces were found to delay

biofilm formation up to 6 days and exhibited more recalcitrance towards *Staphylococcus epidermidis* biofilm formation. It was believed that micro-sized pockets formed by the intertwined nanowires may result in the entrapment of bacterial cells which prevented their crosstalk and proliferation.[280] The advantage of hydrothermal treatments are that they can be easily applied to porous Ti substrates.[292] Nano-flowers, rods and wires were formed in porous Ti alloy scaffolds using an aqueous mixture of calcium hydroxide [$Ca(OH)_2$] and sodium tripolyphosphate [STPP] depending on their ratios and hydrothermal conditions. Nanowire surfaces exhibited bactericidal properties against *Staphylococcus aureus* and *Escherichia coli* as well as osteogenesis from bone cells. Similarly, nanowire surfaces were generated on Ti alloy substrates using a controlled thermal oxidation method, which also showed bactericidal[284] and osteogenic[293] properties. Crucially, this method could be applied to porous and complex shaped Ti substrates, which paves the way to develop cell-instructive nanotopographies for implant applications.

Other fabrication methods have been investigated to produce nanostructured surfaces on Ti substrates. Sengstock *et al.* reported Ti nanocolumnar structures produced using a glancing angle sputter deposition (GLAD) technique. It was again observed that there was more killing of Gram-negative rod-shaped *Escherichia coli* than the Gram-positive sphere-shaped *Staphylococcus aureus*. Apart from their cell wall differences discussed before, their different cell viability on the nanocolumnar structures may also be resulted from their difference in the structural process of cell division. Rod-shaped *Escherichia coli* bacteria multiply by elongating which requires an in-plane movement of the cell body attached to the nanostructures, by which the friction forces during cell dividing dynamics may lead to the damage or disruption of cell wall. In contrast, cell divisions of sphere-shaped *Staphylococcus aureus* occur in three dimensions, with the daughter cells remaining nearby leading to grape-like clusters or out-of-plane growth, which resulted in fewer daughter cells in direct contact with the nanocolumnar surface during cell division process, therefore causing less damage to the cell wall by the friction force.[282] Analogous to black silicon, Hasan *et al.* reported the generation of Ti nanopillars or black Ti (bTi) using a chlorine based reactive ion etching technique. Within 4 hours of contact with the bTi surface, $95\% \pm 5\%$ of *Escherichia coli*, $98\% \pm 2\%$ of *Pseudomonas aeruginosa*, $92\% \pm 5\%$ of *Mycobacterium smegmatis* and $22\% \pm 8\%$ of *Staphylococcus aureus* cells that had attached were killed. The killing efficiency for the *Staphylococcus aureus* increased to $76\% \pm 4\%$ when the bacterial cells were allowed to adhere up to 24 hours.[283]

Polymers are also widely used in medical devices such as catheters, feeding tubes, contact lenses, dental prostheses and orthopedic implants. Nanopatterned surfaces can be fabricated using nanoimprinting and colloidal lithography, both are line-of-sight 2D processes. Dickson *et al.* found that nanopillars replicated from imprinting of lithographically produced moulds and cicada wings were bactericidal against *Escherichia coli*. Sharper, more closely packed nanopillars were more effective, possibly because bacteria on these surfaces both contacted more nanopillars and experienced higher stresses at these contact points,[285] which was in agreement with that found in different insect species.[263] Replication of moth eye-like nanopillars/cones via nanoimprinting also demonstrated good bactericidal performance in both dry and wet conditions,[286,287] which could potentially be used for inhibiting nosocomial infections or any sanitation-conscious touching surfaces. Hazzel *et al*. produced similar nanopillar/cone surfaces using colloidal microbeads as masks followed by RIE. It was shown again that surfaces with the most densely packed nanopillar/cone arrays (center-to-center spacing of 200 nm), higher aspect ratios (<3) and sharp tip widths (>20 nm) killed the highest percentage of bacteria (~30 %).[288].

It is worth noting that the exact mechanisms of bacteria-killing by nanostructures are still not completely clear. One of the most-widely accepted mechanisms is the physical deformation or rupturing of bacterial cell wall/membrane by sharp nanopillars.[262] However, other mechanisms cannot be ruled out, depending on the nano-feature size and structural process of bacterial cell division. For example, the physical entrapment of bacteria within nanopillars or nanowires may impede the proliferation and growth of bacteria.[280] The friction forces exerted on the Gram-negative bacterial cell wall during their division process may also result in the damage of bacterial cell wall.[282] It is therefore important to elucidate the nanotopography-induced antibacterial mechanisms in order to rationally design and fabricate nanostructures for relevant biomedical applications.

6. Cell-instructive (osteogenic and antibacterial) nanotopographies

For many biomedical applications, surfaces with cell-instructive or cell-selective functionalities that are able to control the fate of both mammalian and bacterial cells at the same time are highly desirable. As previously discussed, orthopaedic implants provide a good example of a sector requiring cell-instructive surfaces that could simultaneously promote osseointegration and prevent bacterial infection. This is because the increased demand for orthopaedic prosthesis

is fueled by both aseptic loosening (due to poor osseointegration) or infection (due to bacterial infiltration and biofilm formation).[10,294]

The use of topographical cues to selectively modulate cells and bacteria has becoming increasingly reported on, mostly on pure Ti metal and its alloys (e.g. Ti6Al4V) because they are most widely used materials for endosseous implants. For example, Peng et al. reported that concave nanotopographies e.g. TiO_2 nanotube arrays with diameters of 30 to 80 nm grown on Ti substrates via anodization exhibited reduced adhesion and lower colonization of bacterial cells (*Staphylococcus epidermidis*) but enhanced, increased, adhesion of osteogenic cells.[143] Similar cell-selective behavior was observed on nanoporous surfaces for human gingival FBs and oral bacteria (*Streptococcus mutans*, *Fusobacterium nucleatum* and *Porphyromonas gingivalis*).[295] Different cell-selective behavior has also been reported on convex nanotopographies. Densely packed Ti nanocolumns with diameters of 40 to 60 nm fabricated via glancing angle deposition (GLAD) showed strongly reduced bacterial (*Staphylococcus aureus*) adhesion and biofilm formation, while osteoblast cells grew well on such surfaces. The selective cell behaviors were attributed to the 'lotus leaf effect' caused by the nanocolumnar arrays and the difference in the dimensions of osteoblast and bacterial cells.[144]

Since the recent discovery of high aspect ratio bactericidal nanotopographies as reviewed in part 5, research has been carried out on selective cellular responses of both mammalian cells (OBs, MSCs and other cells) and bacteria to such surfaces. The group of Ivanova demonstrated, for example, that while bSi surfaces killed bacteria, the COS-7 eukaryotic cell model could survive and grow.[296] In fact, the bactericidal nanotopographies, fabricated from bSi with densely packed nanoneedles, promoted the growth and proliferation of fibroblastic cells. Such nanotopography was not only biocompatible but also reduced inflammatory response in a mice model compared with the flat controls.[296] For orthopaedic application, however, we need to consider bone forming cells. Diu et al. noted that the metabolic activity of OB (MG63) cells cultured on bactericidal hydrothermal TiO_2 nanowire surfaces was only slightly decreased after 14 days of cell culture and that while proliferation of OB cells was slowed, especially on long TiO_2 nanowires that formed secondary 'pocket' structures, the cells did grow with time. A noticeable change in cell morphology was that some cells became elongated due to 'pinning' of osteoblast cells on bactericidal TiO_2 nanowire arrays.[278] Similar results were reported from other groups using different materials or other cell lines.[279,281,283]

Most interestingly, these convex high-aspect-ratio, bactericidal nanotopographies seem capable of directing the differentiation of MSCs into OBs, which could have positive implication to the

real-world applications in orthopaedic or dental implants where both antimicrobial and osseointegrative properties are vital to ensure their long-term success. Tsimbouri et al. investigated osteogenesis of bactericidal TiO_2 nanowires using a mesenchymal bone marrow stromal cell (BMSC)/bone marrow hematopoietic cell (BMHC) co-culture model where both osteogenesis and osteoclastogenesis can occur.[297]

Similar to the previous results,[278] BMSCs were well-spread on shorter 'fine' or 'brush' nanowire surfaces (2 hours (2h) of anodization) with well-organized cytoskeleton but grew slight less well compared with the polished control. Nevertheless, cell proliferation was impaired when growing on longer 'coarse' or 'niche' nanowire surfaces (>2h) (Figure 10). Cells tended to 'trap' inside the pockets formed by the intertwined nanowires. Interestingly, analysis of osteogenic markers osteopontin (OPN) and osteocalcin (OCN) at the transcript and protein level demonstrated an increase in osteogenesis on the 2h nanowire surface compared with the polished control. This indicated that such a surface could be both bactericidal and osteogenic, thus potentially useful in the development of cell-instructive implants. It is notable that the nanowires also prevented osteoclastogenesis and this could have implication in reducing osteolysis.

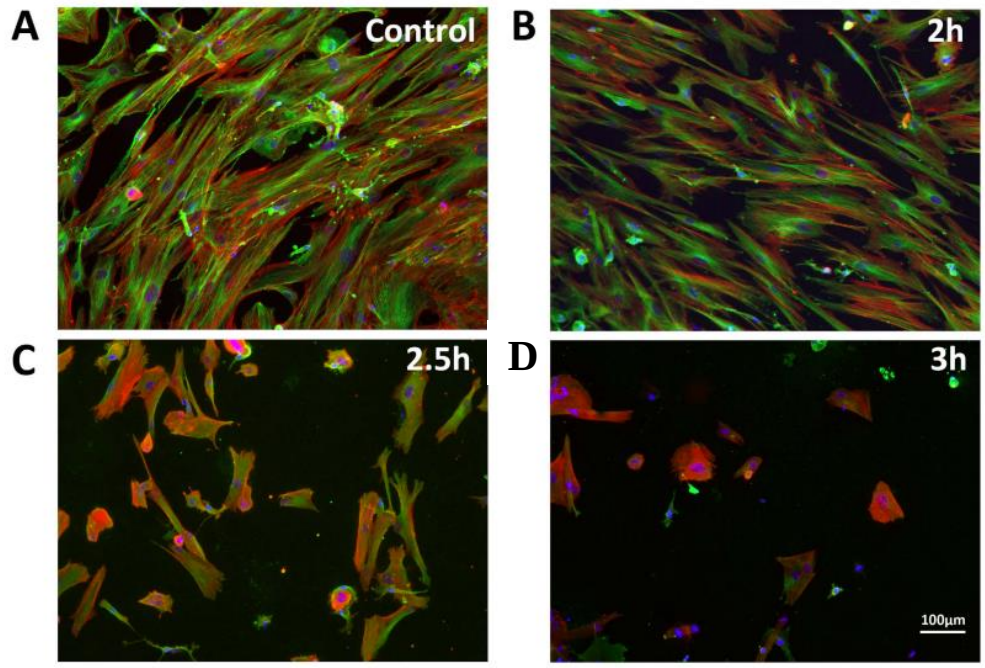

Figure 10. Immunofluorescence micrographs showing cell morphology and spread for BMSCs cultured on different bactericidal TiO_2 nanotopographies. (A) flat control, (B) 2h, (C) 2.5h and (D) 3h surfaces (the length of anodization increasing nanowire size). Notable is that cells on the 2h nanowires spread

well – similar to on planar control. Red: actin, Green: tubulin, Blue: nucleus. Reproduced under the terms of the Creative Commons Attribution-NonCommercial-NoDerivatives 4.0 International license (CC BY-NC-ND 4.0).[278] Copyright 2014, Springer Nature.

7. The synergy of nanotopography and chemical coatings

Nanotopographies with bactericidal potential and capacity to support bone cells populations would be ideal substrates for developing new medical implants, and the recent literature indicates this is possible (see previous Section). However, it is difficult to design cell instructive surfaces with topography alone, i.e. there is typically a reduction in spreading and/or proliferation of bone-related cell types on high aspect ratio bactericidal topographies compared to control Ti surfaces.[278,283,297] A potential solution to achieve this would be the functionalization of such high aspect-ratio antibacterial topographies with chemical ligands with integrin-binding potential. As discussed in Section 4, it is important for bone forming cells to form "super-mature" focal adhesions (> 5 μm long) in order to stabilize the large OB morphology and thus promote osteogenesis. Thus, a combined topography-chemistry approach could improve cell function on less adherent surfaces.

Fraioli et al. further investigated the use of peptidic ligands combined with bactericidal TiO_2 nanotopographies to improve integrin-specific cell adhesion and hopefully enhance osteogenesis (Figure 11).[298] It was indeed observed that the functionalization of nanowires by the integrin-binding molecules improved MSCs adhesion significantly (Figure 11C), with increased cell area and formation of larger focal adhesions, which are required for bone formation. Notably, this effect was observed even on the spiky 3h anodization 'coarse' nanowire surface, where very poor cell adhesion and proliferation was initially found (Figure 10D).[278] Further, the study of osteogenic markers confirmed a moderate increase in osteogenesis on the αvβ3-integrin selective peptidomimetic-functionalized nanotopographies. Crucially, the bactericidal properties of the high-aspect-ratio nanotopographies have not been masked by the integrin-binding molecules.

Thus, the functionalization of nanostructured surfaces with chemical coatings should be regarded as a way to improve their cell instructive properties, and offers the possibility to further introduce a wide range of biological activities, which may not be always attainable by topography alone. We showed MSC response can be improved with integrin-binding ligands, while keeping antimicrobial effects; but many other biochemical cues may be introduced, e.g. GFs and osteogenic peptides, mineralization sequences, and even AMPs or other antibacterial

agents. These molecules may be incorporated using covalent (irreversible) approaches or drug-releasing systems, as we have described in Sections 3.1 and 3.2. Another particularly relevant strategy would be to employ stimuli-responsive linkers, which could be cleaved upon enzymatic activity by either eukaryotic cells[299] or bacteria,[300] releasing or exposing the desired function in a dynamic and smart fashion. The possibilities are enormous and have not been investigated yet.

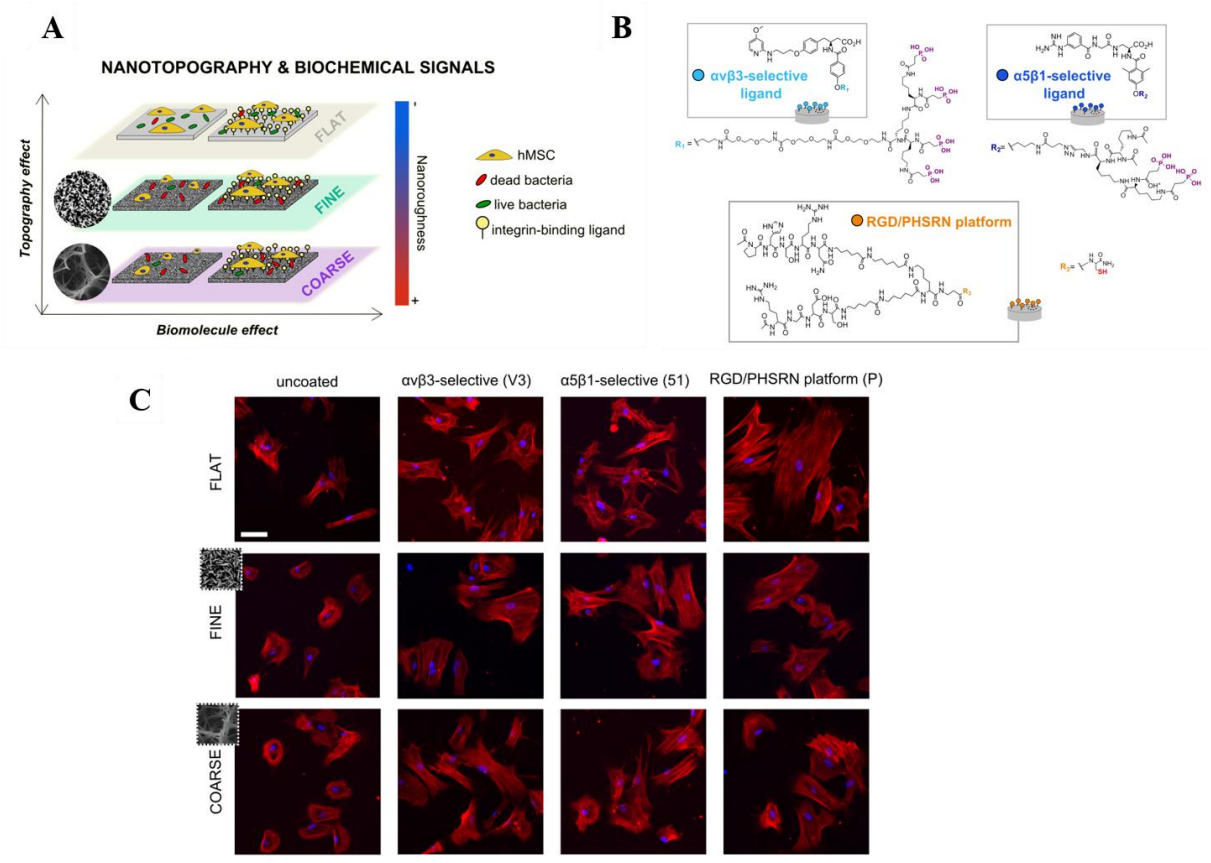

Figure 10. A) Combining topographical and biochemical cues on the surface of biomaterials allows for a dual cell adhesive and antibacterial effect; B) Chemical structure of the synthetic ligands: αvβ3-selective (V3) or α5β1-selective (51) peptidomimetics,[70] and a peptidic platform combining RGD/PHSRN (P) [78,79]); C) Immunostained actin fibers and DAPI-stained nuclei for the flat control, fine and coarse nanotopographies functionalized with the three different integrin-binding molecules (V3, 51, or P). Scale bar=100 μm. Reproduced (adapted) under the terms of the Creative Commons Attribution 4.0 International license (CC BY 4.0).[298] Copyright 2017, Springer Nature.

8. Conclusions

In this review we have shown that both chemical and topographical cues are potent modulators of the functions of eukaryotic and prokaryotic cells. In this regard, modifying the biomaterial surface properties to simultaneously enhance host cell adhesion and function while inhibiting bacterial biofilm formation has been a major focus; we have reported recent strategies that demonstrate this is possible. However, as more efforts are put into developing novel methodologies, the number of challenges increases too.

In the first place, it is becoming evident that the biological evaluation of the osteoconductive and antibacterial potential of any new multifunctional surface will require the use of eukaryotic cell-bacteria co-cultures, as the results obtained with the individual cell types may greatly differ from the more realistic, competitive scenario. In a recent study, we showed that bacteria directly inhibited the capacity of osteoblastic cells to spread and proliferate.[184] This study indicates that bacteria and cells not only race for the surface, but 'fight for it', and makes us postulate that the interactions between these two cell types and the biomaterial surface are better referred to as "the fight for the surface". However, the mechanisms governing these interactions are not well understood, as the majority of current methods focus on the 'finish line',[14] but do not monitor the dynamic process of competition for the surface. Coupling biomaterials science with biosensing technologies could help to take a step forward to better understand this process.

Achieving potent osteogenic effects on the biomaterial surface is another challenge. Cell adhesive peptides such as RGD have shown moderate to poor outcomes in animal studies;[71,72,73] and the delivery of GFs like BMPs, while very effective in inducing bone formation, has raised concerns with regard to unwanted side effects, thus hampering its widespread clinical application.[90,91] Recent progress on developing multifunctional systems synergizing integrin and GF signaling have shown it is possible to achieve excellent osteogenic responses *in vitro* and bone growth *in vivo*, with only very low doses of GFs.[86,87,88,89] Such systems may likely represent future strategies for implant-driven osteoinduction. The development of GF-derived, short synthetic peptides and mimetics holds great potential too, and has not been fully explored. The combination of osteogenic peptides with antibacterial agents, like AMPs, has not been investigated either.

We have also discussed that an increasing concern in the medical device arena is the emergence of bacterial resistance. However, most approaches to fight infections on biomaterials still rely on the use of antibiotics. While is true that newer systems of drug-delivery are being developed, with much better and improved release kinetics, replacement of antibiotics by other

antibacterial systems, like the immobilization of AMPs, needs to be further studied. Moreover, some other frequent strategies used in biomaterials research present limitations too. This is the case, for example, of silver, one of the 'gold standards' for use in antibacterial surfaces, but that presents toxicity for eukaryotic cells. In response to these limitations, innovations in genomics and the identification of new sources of antibacterial potential are being proposed to fill the classic antibacterial agents gap.[301, 302] Interfering with bacterial quorum sensing communication is another emerging strategy with potential to inhibit biofilm formation on biomaterials.[303] Incorporation of such novel antibacterial drugs on biomaterials might well decrease the risk of bacterial resistance.

Finally, conferring osteogenic or antibacterial potential to surfaces by pure topographical effects opens up new and promising possibilities in GF- and antibiotic-free medical therapies. Further, achieving both effects by means of topography is a very promising avenue of research and we have shown this is feasible. However, we also acknowledge that this strategy may be limited in terms of bioactivity: the same way bacteria and eukaryotic cells are different in size and morphology, the nanopatterns that maximize one biological effect (e.g. osteogenesis) are in general different from those required to exert the other one (e.g. bacterial kill). This is illustrated by several antibacterial nanopatterns, such as high aspect-ratio surfaces, which effectively kill bacteria, but reduce MSCs functions at the same time. However, we have shown that chemical functionalization of nanotopographies with integrin-binding molecules is a viable way to overcome this hurdle.[298] Thus, functionalizing nanotopographies with cell adhesive or antibacterial peptides opens new horizons towards highly cell instructive multifunctional biomaterials. The physical bacterial killing mechanism represented by topography is likely to be more evolution resistant than drug-based strategies and the chemical approach can help drive osteogenesis while maintaining bacterial kill. This approach offers an unlimited combination of biological signals for a wide range of applications, and, interestingly, only now is starting to be investigated.

Acknowledgements

C.M.-M wants to thank the Spanish Government for financial support through a Ramon y Cajal grant (RYC-2015-18566) and Projects No. MAT2015-67183-R and MAT2017-83905-R (MINECO/FEDER), co-funded by the European Union through European Regional Development Funds, the Government of Catalonia (2017 SGR1165) and the European Commission for a Marie Curie Career Integration Grant (REA Grant Agreement No. 321985). M.J.D. thanks the EPSRC for grant EP/K034898/1.

Received: ((will be filled in by the editorial staff))
Revised: ((will be filled in by the editorial staff))
Published online: ((will be filled in by the editorial staff))

References

[1] M. L. Wolford, K. Palso, A. Bercovitz, Hospitalization for total hip replacement among inpatients aged 45 and over: United States, 2000–2010. NCHS data brief, no 186. Hyattsville, MD: National Center for Health Statistics. 2015.

[2] S. N. Williams, M. L. Wolford, A. Bercovitz, Hospitalization for total knee replacement among inpatients aged 45 and over: United States, 2000–2010. NCHS data brief, no 210. Hyattsville, MD: National Center for Health Statistics. 2015.

[3] S. Kurtz, K. Ong, E. Lau, F. Mowat, M. Halpern, *J. Bone Joint Surg. Am*. **2007**, *89*, 780.

[4] OECD/EU (2016), Health at a Glance: Europe 2016 – State of Health in the EU Cycle, OECD Publishing, Paris. http://dx.doi.org/10.1787/9789264265592-en.

[5] L. Leitner, S. Türk, M. Heidinger, B. Stöckl, F. Posch, W. Maurer-Ertl, A. Leithner, P. Sadoghi, *Sci. Reports* **2018**, *8*, 4707.

[6] J. A. Bishop, A. A. Palanca, M. J. Bellino, D. W. Lowenberg, *J. Am. Acad. Orthop. Surg*. **2012**, 20, 273.

[7] H. T. Aro, J. J. Alm, N., Moritz, T. J. Makinen, P. Lankinen, *Acta Orthop*. **2012**, 83, 107.

[8] S. Kurtz, F. Mowat, K. Ong, N. Chan, E. Lau, M. Halpern, *J. Bone Joint Surg. Am*. **2005**, 87, 1487.

[9] S. B. Goodman, Z. Yao, M. Keeney, F. Yang, *Biomaterials* **2013**, *34*, 3174.

[10] J. Raphel, M. Holodniy, S. B. Goodman, S. C. Heilshorn, *Biomaterials* **2016**, *84*, 301.

[11] R. E. Delanois, J. B. Mistry, C. U. Gwam, N. S. Mohamed, U. S. Choksi, M. A. Mont, *J. Arthroplasty* **2017**, 32, 2663.

[12] R. Adell, U. Lekholm, B. Rockler, P. I Brånemark, *Int. J. Oral Surg*. **1981**, *10*, 387.

[13] C. Mas-Moruno, M. Espanol, E. B. Montufar, G. Mestres, C. Aparicio, F. J. Gil, M. P. Ginebra, in *Biomaterials Surface Science* (Eds: A. Taubert, J. F. Mano, J. C Rodríguez-Cabello), Wiley-VCH, Weinheim, Germany **2013**, pp. 337-374.

[14] H. J. Busscher, H. C. van der Mei, G. Subbiahdoss, P. C. Jutte, J. J. M. van denDungen, S. J. Zaat, M. J. Schultz, D. W. Grainger, *Sci. Transl. Med*. **2012**, *4*, 153rv10.

[15] S. Veerachamy, T. Yarlagadda, G. Manivasagam, P. K. Yarlagadda, Bacterial adherence and biofilm formation on medical implants: a review. *Proc. Inst. Mech. Eng. H J. Eng. Med*. **2014**, *228*, 1083.

[16] E. T. J. Rochford, R. G. Richards, T. F. Moriarty, *Clin. Microbiol. Infect.* **2012**, *18*, 1162.

[17] P. E. Kolenbrander, R. J. Palmer, S. Periasamy, N. S. Jakubovics, *Nat. Rev. Microbiol*. **2010**, *8*, 471.

[18] C. R. Arciola, D. Campoccia, P. Speziale, L. Montanaro, J. W. Costerton, *Biomaterials* **2012**, *33*, 5967.

[19] A. H. Holmes, L. S. P. Moore, A. Sundsfjord, M. Steinbakk, S. Regmi, A. Karkey, P. J. Guerin, L. J. V. Piddock, *Lancet* **2016**, *387*, 176.

[20] W. Costerton, R. Veeh, M. Shirtliff, M. Pasmore, C. Post, G. Ehrlich, *J. Clin. Invest*. **2003**, *112*, 1466.

[21] A. Lee, H. L. Wang, *Implant Dent.* **2010**, 19, 387.

[22] R. P. Darveau, *Nat. Rev. Microbiol*. **2010**, *8*, 481.

[23] K. Vasilev, J. Cook, H. J. Griesser, *Expert Rev. Med. Devices* **2009**, *6*, 553.

[24] P. A. Norowski, J. D. Bumgardner, *J. Biomed. Mater. Res. − Part B Appl. Biomater*. **2009**, *88*, 530.

[25] M. A. Fernandez-Yague, S. A. Abbah, L. McNamara, D. I. Zeugolis, A. Pandit, M. J. Biggs, *Adv. Drug Deliver. Rev*. **2015**, *84*, 1.

[26] S. Bauer, P. Schmuki, K. von der Mark, J. Park, *Prog. Mater. Sci.* **2013**, *58*, 261.

[27] A. Shekaran, A. J. Garcia, *J. Biomed. Mater. Res. A* **2011**, *96*, 261.

[28] R. Tejero, E. Anitua, G. Orive, *Prog. Polym. Sci*. **2014**, *39*, 1406.

[29] A. Civantos, E. Martínez-Campos, V. Ramos, C. Elvira, A. Gallardo, A. Abarrategi, *ACS Biomater. Sci. Eng*. **2017**, *3*, 1245.

[30] I. Banerjee, R. C. Pangule, R. S. Kane, *Adv. Mater*. **2011**, *23*, 690.

[31] K. Glinel, P. Thebault, V. Humblot, C. M. Pradier, T. Jouenne, *Acta Biomater*. **2012**, *8*, 1670.

[32] L. Zhang, C. Ning, T. Zhou, X. Liu, K. W. K. Yeung, T. Zhang, Z. Xu, X. Wang, S. Wu, P. K. Chu, *ACS Appl. Mater. Interfaces* **2014**, *6*, 17323.

[33] E. M. Hetrick, M. H. Schoenfisch, *Chem. Soc. Rev*. **2006**, *35*, 780.

[34] N. J. Hickok, I. M. Shapiro, *Adv. Drug Deliv. Rev*. **2012**, *64*, 1165.

[35] C. Mas-Moruno, in *Peptides and Proteins as Biomaterials for Tissue Regeneration and Repair* (Eds: M. A. Barbosa, M. C. L. Martins), Elsevier, Woodhead Publishing, **2018**, pp. 73-100.

[36] K. G. Neoh, X. Hu, D. Zheng, E. T. Kang, *Biomaterials* **2012**, *33*, 2813.

[37] S. Spriano, S. Yamaguchi, F. Baino, S. Ferraris, *Acta Biomater*. **2018**, *79*, 1.

[38] A. G. Gristina, *Science* **1987**, *237*, 1588.

[39] L. Le Guéhennec, A. Soueidan, P. Layrolle, Y. Amouriq, *Dental Mater*. **2007**, *7*, 844.

[40] B. D. Bovan, T. W. Hummert, D. D. Dean, Z. Schwartz, *Biomaterials* **1996**, *17*, 137.

[41] J. Y. Martin, Z. Schwartz, T. W. Hummert, D. M. Schraub, J. Simpson, J. Jr. Lankford, D. D. Dean, D. L. Cochran, B. D. Boyan, *J. Biomed. Mater. Res*. **1995**, *29*, 389.

[42] M. Pegueroles, C. Aparicio, M. Bosio, E. Engel, F. J. Gil, J. A. Planell, G. Altankov, *Acta Biomater*. **2010**, *6*, 291.

[43] C. M. Bollen, W. Papaioanno, J. Van Eldere, E. Schepers, M. Quirynen, D. van Steenberghe, *Clin. Oral Implants Res*. **1996**, *7*, 201.

[44] D. D. Deligianni, N. Katsala, S. Ladas, D. Sotiropoulou, J. Amedee, Y. F. Missirlis, *Biomaterials* **2001**, *22*, 1241.

[45] K. de Groot, R. Geesink, C. P. Klein, P. Serekian, *J. Biomed. Mater. Res.* **1987**, *21*, 1375.

[46] F. Barrere, C. M. van der Valk, G. Meijer, R. A. Dalmeijer, K. de Groot, P. Layrolle, *J. Biomed. Mater. Res.* **2003**, *67*, 655.

[47] R. G. T. Geesink, K. de Groot, C. P. A. T. Klein, *Clin. Orthop*. **1987**, *225*, 147.

[48] M. Shrikhanzadeh, *J. Mater. Sci. Lett.* **1991**, *10*, 1415.

[49] J. E. Hulshoff, T. Hayakawa, K. van Dijk, A. F. Leijdekkers-Govers, J. P. van der Waerden, J. A. Jansen, *J. Biomed. Mater. Res*. **1997**, *36*, 75.

[50] J. Lee, L. Rouhfar, O. Beirne, *J. Oral Maxillofac. Surg*. **2000**, *58*, 1372.

[51] T. Kokubo, F. Miyaji, H. M. Kim, *J. Amer. Ceram. Soc.* **1996**, *79*, 1127.

[52] H. B. Wen, J. R. De Wijn, Q. Liu, K. De Groot, F. Z. Cui, *J. Mater. Sci. Mater. Med*. **1997**, *8*, 765.

[53] P. Li, K. De Groot *J. Biomed. Mater. Res.* **1993**, *27*, 1445.

[54] A. A. Campbell, G. Fryxell, J. Linehan, G. *J. Biomed. Mater. Res*. **1996**, *32*, 111.

[55] C. Ohtsuki, H. Iida, S. Hayakawa, A. Osaka, *J. Biomed. Mater. Res*. **1997**, *35*, 39.

[56] P. Li, P. Ducheyne, *J. Biomed. Mater. Res.* **1998**, *41*, 341.

[57] X. Wang, W. Yan, S. Hayakawa, K. Tsuru, A. Osaka, *Biomaterials* **2003**, *24*, 4631.

[58] S. Nishiguchi, H. Kato, H. Fujita, M. Oka, H. M. Kim, T. Kokubo, T. Nakamura, *Biomaterials* **2001**, *22*, 2525.

[59] T. Miyaza, H. M. Kim, T. Kokubo, C. Ohtsuki, H. Kato, T. Nakamura, *Biomaterials* **2002**, *23*, 827.

[60] M. Uchida, H. M. Kim, F. Miyaji, T. Kokubo, T. Nakamura, *Biomaterials* **2002**, *23*, 313.

[61] T. Kokubo, H. M. Kim, M. Kawashita, T. Nakamura, *J. Mater. Sci. Mater. Med*. **2004**, *15*, 99.

[62] G. Bhardwaj, H. Yazici, T. J. Webster, *Nanoscale* **2015**, *7*, 8416.

[63] M. P. Ginebra, C. Canal, M. Espanol, D. Pastorino, E. B. Montufar, *Adv. Drug Deliv. Rev*. **2012**, *64*, 1090.

[64] A. E. Rodda, L. Meagher, D. R. Nisbet, J. S. Forsythe, *Prog. Polym. Sci*. **2014**, *39*, 1312.

[65] K. von der Mark, J. Park, *Prog. Mater. Sci*. **2013**, *58*, 327.

[66] M. D. Pierschbacher, E. Ruoslahti, *Nature* **1984**, *309*, 30.

[67] M. D. Pierschbacher, E. Ruoslahti, *Cell* **1986**, *44*, 517.

[68] R. O. Hynes, *Cell* **2002**, *110*, 673.

[69] U. Hersel, C. Dahmen, H. Kessler, *Biomaterials* **2003**, *24*, 4385.

[70] C. Mas-Moruno, R. Fraioli, F. Rechenmacher, S. Neubauer, T. G. Kapp, H. Kessler, *Angew. Chem. Int. Ed.* **2016**, *55*, 7048.

[71] S. L. Bellis, *Biomaterials* **2011**, 32, 4205.

[72] T. H. Barker, *Biomaterials* **2011**, *32*, 4211.

[73] J. H. Collier, T. Segura, *Biomaterials* **2011**, *32*, 4198.

[74] T. A. Petrie, J. R. Capadona, C. D. Reyes, A. J. Garcia, *Biomaterials* **2006**, *27*, 5459.

[75] T. A. Petrie, J. E. Raynor, C. D. Reyes, K. L. Burns, D. M. Collard, A. J. García, *Biomaterials* **2008**, *29*, 2849.

[76] R. Agarwal, C. González-García, B. Torstrick, R. E. Guldberg, M. Salmerón-Sánchez, A. J. García, *Biomaterials* **2015**, 63, 137.

[77] C. Herranz-Diez, C. Mas-Moruno, S. Neubauer, H. Kessler, F. J. Gil, M. Pegueroles, J. M. Manero, J. Guillem-Marti, *ACS Appl. Mater. Interfaces* **2016**, *8*, 2517.

[78] C. Mas-Moruno, R. Fraioli, F. Albericio, J. M. Manero, F. J. Gil, *ACS Appl. Mater. Interfaces* **2014**, *6*, 6525.

[79] R. Fraioli, K. Dashnyam, J. H. Kim, R. A. Perez, H. W. Kim, J. Gil, M. P. Ginebra, J. M. Manero, C. Mas-Moruno, *Acta Biomater.* **2016**, 43, 269.

[80] M. Pagel, R. Hassert, T. John, K. Braun, M. Wießler, B. Abel, A. G. Beck-Sickinger, *Angew. Chemie Int. Ed.* **2016**, *55*, 4826.

[81] R. Fraioli, F. Rechenmacher, S. Neubauer, J. M. Manero, J. Gil, H. Kessler, C. Mas-Moruno, *Colloid. Surf. B.* **2015**, *128*, 191.

[82] B. Bragdon, O. Moseychuk, S. Saldanha, D. King, J. Julian, A. Nohe, *Cell. Signal.* **2011**, *23*, 609.

[83] Q. Wei, T. L. M. Pohl, A. Seckinger, J. P. Spatz, E. A. Cavalcanti-Adam, *Beilstein J. Org. Chem.* **2015**, *11*, 773.

[84] M. Salmerón-Sánchez, M. J. Dalby, *Chem. Commun.* **2016**, *52*, 13327.

[85] M. M. Martino, P. S. Briquez, K. Maruyama, J. A. Hubbell, *Adv. Drug Deliv. Rev.* **2015**, *94*, 41.

[86] M. Kisiel, M. M. Martino, M. Ventura, J. A. Hubbell, J. Hilborn, D. A. Ossipov, *Biomaterials* **2013**, *34*, 704.

[87] M. M. Martino, F. Tortelli, M. Mochizuki, S. Traub, D. Ben-David, G. A. Kuhn, R. Muller, E. Livne, S. A. Eming, J. A. Hubbell, *Sci. Transl. Med.* **2011**, *3*, 100ra89.

[88] A. Shekaran, J. R. García, A. Y. Clark, T. E. Kavanaugh, A. S. Lin, R. E. Guldberg, A. J. García, *Biomaterials* **2014**, *35*, 5453.

[89] V. Llopis-Hernández, M. Cantini, C. González-García, Z. A. Cheng, J. Yang, P. M. Tsimbouri, A. J. García, M. J. Dalby, M. Salmerón-Sánchez, *Sci Adv.* **2016**, *2*, e1600188.

[90] E. J. Carragee, E. L. Hurwitz, B. K. A. Weiner, *Spine J.* **2011**, *11*, 471.

[91] E. J. Carragee, G. Chu, R. Rohatgi, E. L. Hurwitz, B. K. Weiner, S. T. Yoon, G. Comer, B. Kopjar, *J. Bone Joint Surg. Am.* **2013**, *95*, 1537.

[92] T. Fowler, E. R. Wann, D. Joh, S. Johansson, T. J. Foster, M. Höök, *Eur. J. Cell Biol.* **2000**, *79*, 672.

[93] U. Schwarz-Linek, J. M. Werner, A. R. Pickford, S. Gurusiddappa, J. H. Kim, E. S. Pilka, J. A. Briggs, T. S. Gough, M. Höök, I. D. Campbell, J. R. Potts, *Nature* **2003**, *423*, 177.

[94] J. M. Patti, J. O. Boles, M. Hook, *Biochemistry* **1993**, *32*, 11428.

[95] C. Aparicio, F. J. Gil, C. Fonseca, M. Barbosa, J. A. Planell, *Biomaterials* **2003**, *24*, 263.

[96] C. Aparicio, J. M. Manero, F. Conde, M. Pegueroles, J. A. Planell, M. Vallet-Regi, F. J. Gil, *J. Biomed. Mater. Res. A* **2007**, *82*, 521.

[97] C. Aparicio, F. J. Gil, J. A. Planell, E. Engel, *J. Mater. Sci. Mater. Med.* **2002**, *13*, 1105.

[98] C. Aparicio, A. Padros, F. J. Gil, *J. Mech. Behav. Biomed. Mater*. **2011**, *4*, 1672.

[99] C. Mas-Moruno, P. M. Dorfner, F. Manzenrieder, S. Neubauer, U. Reuning, R. Burgkart, H. Kessler, *J. Biomed. Mater. Res. Part A* **2013**, *101*, 87.

[100] K. G. Neoh, E. T. Kang, *ACS Appl. Mater. Interfaces* **2011**, *3*, 2808.

[101] O'Neill, J. Tackling drug-resistant infections globally: final report and recommendations. The review on antimicrobial resistance. May 2016. Wellcome Trust. London, UK.

[102] S. Buffet-Bataillon, P. Tattevin, M. Bonnaure-Mallet, A. Jolivet-Gougeon, *Int. J. Antimicrob. Agents* **2012**, *39*, 381.

[103] K. Hiramatsu, Y. Katayama, M. Matsuo, T. Sasaki, Y. Morimoto, A. Sekiguchi, T. Baba, *J. Infect. Chemother*. **2014**, *20*, 593.

[104] O. Bondarenko, K. Juganson, A. Ivask, K. Kasemets, M. Mortimer, A. Kahru, *Arch. Toxicol*. **2013**, *87*, 1181.

[105] N. Duewelhenke, O. Krut, P. Eysel, *Antimicrob. Agents Chemother*. **2007**, *51*, 54.

[106] L. G. Harris, S. Tosatti, M. Wieland, M. Textor, R. G. Richards, *Biomaterials* **2004**, *25*, 4135.

[107] R. R. Maddikeri, S. Tosatti, M. Schuler, S. Chessari, M. Textor, R. G. Richards, L. G. Harris, *J. Biomed. Mater. Res. Part A* **2008**, *84*, 425.

[108] G. Subbiahdoss, B. Pidhatika, G. Coullerez, M. Charnley, R. Kuijer, *Eur. Cells Mater.* **2010**, *19*, 205.

[109] J. Buxadera-Palomero, C. Calvo, S. Torrent-Camarero, F. J. Gil, C. Mas-Moruno, C. Canal, D. Rodríguez, *Colloid Surf. B Biointerfaces* **2017**, *152*, 367.

[110] Z. Shi, K. G. Neoh, E. T. Kang, C. Poh, W. Wang, *Tissue Eng. Part A* **2009**, *15*, 417.

[111] F. Zhang, Z. Zhang, X. Zhu, E. T. Kang, K. G. Neoh, *Biomaterials* **2008**, *29*, 4751.

[112] X. Hu, K. G. Neoh, Z. Shi, E. T. Kang, C. Poh, W. Wang, *Biomaterials* **2010**, *31*, 8854.

[113] Q. Yu, Z. Wu, H. Chen, *Acta Biomater*. **2015**, *16*, 1.

[114] S. Yan, L. Song, S. Luan, Z. Xin, S. Du, H. Shi, S. Yuan, Y. Yang, J. Yin, *Colloids Surf. B Biointerfaces* **2017**, *150*, 250.

[115] J.-B. Paris, D. Seyer, T. Jouenne, P. Thébault, *Colloids Surf. B Biointerfaces* **2017**, *156*, 186.

[116] Q. Gao, M. Yu, Y. Su, M. Xie, X. Zhao, P. Li, P.X. Ma, *Acta Biomater*. **2017**, *51*, 112.

[117] C. Yang, X. Ding, R.J. Ono, H. Lee, L.Y. Hsu, Y.W. Tong, J. Hedrick, Y.Y. Yang, *Adv. Mater*. **2014**, *26*, 7346.

[118] Y. Su, Z. Zhi, Q. Gao, M. Xie, M. Yu, B. Lei, P. Li, P.X. Ma, *Adv. Healthc. Mater*. **2017**, *6*, 1.

[119] Z. Zhi, Y. Su, Y. Xi, L. Tian, M. Xu, Q. Wang, S. Padidan, P. Li, W. Huang, *ACS Appl. Mater. Interfaces* **2017**, *9*, 10383.

[120] M. Dash, F. Chiellini, R.M. Ottenbrite, E. Chiellini, *Prog. Polym. Sci*. **2011**, *36*, 981.

[121] P. Chua, K. Neoh, E. Kang, W. Wang, *Biomaterials* **2008**, *29*, 1412.

[122] Z. Shi, K. G. Neoh, E. T. Kang, C. Poh, W. Wang, *J. Biomed. Mater. Res. Part A.* **2008**, *86*, 865.

[123] Z. Shi, K. G. Neoh, E. T. Kang, C. K. Poh, W. Wang, *Biomacromolecules* **2009**, *10*, 1603.

[124] L. Han, H. Lin, X. Lu, W. Zhi, K.-f. Wang, F.-z. Meng, O. Jiang, *Mater. Sci. Eng. C* **2014**, *40*, 1.

[125] D. Zheng, K. G. Neoh, E. T. Kang, *Appl. Surf. Sci*. **2016**, *360*, 86.

[126] M. A. Bonifacio, S. Cometa, M. Dicarlo, F. Baruzzi, S. de Candia, A. Gloria, M. M. Giangregorio, M. Mattioli-Belmonte, E. De Giglio, *Carbohydr. Polym*. **2017**, *166*, 348.

[127] A. Jain, L. S. Duvvuri, S. Farah, N. Beyth, A. J. Domb, W. Khan, *Adv. Healthcare Mater.* **2014**, *3*, 1969.

[128] R. Ye, H. Xu, C. Wan, S. Peng, L. Wang, H. Xu, Z. P. Aguilar, Y. Xiong, Z. Zeng, H. Wei, *Biochem. Biophys. Res. Commun.* **2013**, *439*, 148.

[129] R. Wang, D.-l. Xu, L. Liang, T.-t. Xu, W. Liu, P.-k. Ouyang, B. Chi, H. Xu, *RSC Adv.* **2016**, *6*, 8620.

[130] R. Wang, J. Li, W. Chen, T. Xu, S. Yun, Z. Xu, Z. Xu, T. Sato, B. Chi, H. Xu, *Adv. Funct. Mater.* **2017**, *27*, 1604894.

[131] Y. Cheng, H. Yang, Y. Yang, J. Huang, K. Wu, Z. Chen, X. Wang, C. Lin, Y. Lai, *J. Mater. Chem. B*, **2018**, *6*, 1862.

[132] K. Das, S. Bose, A. Bandyopadhyay, B. Karandikar, B. L. Gibbins, *J. Biomed. Mater. Res. Part B* **2008**, *87*, 455.

[133] L. Zhao, H. Wang, K. Huo, L. Cui, W. Zhang, H. Ni, Y. Zhang, Z. Wu, P. K. Chu, *Biomaterials* **2011**, *32*, 5706.

[134] A. Gao, R. Hang, X. Huang, L. Zhao, X. Zhang, L. Wang, B. Tang, S. Mad, P. K. Chu, *Biomaterials* **2014**, *35*, 4223.

[135] K. Huo, X. Zhang, H. Wang, L. Zhao, X. Liu, P.K. Chu, *Biomaterials* **2013**, *34*, 3467.

[136] Y. Li, W. Xiong, C. Zhang, B. Gao, H. Guan, H. Cheng, J. Fu, F. Li, *J. Biomed. Mater. Res. Part A* **2014**, *102*, 3939.

[137] R. Hang, A. Gao, X. Huang, X. Wang, X. Zhang, L. Qin, B. Tang, *J. Biomed. Mater. Res. A* **2014**, *102*, 1850.

[138] K. C. Popat, M. Eltgroth, T. J. Latempa, C. A. Grimes, T. A. Desai, *Biomaterials* **2007**, *28*, 4880.

[139] T. Kumeria, H. Mon, M. S. Aw, K., Gulati, A. Santos, H. J. Griesser, D. Losic, *Colloid Surf. B Biointerfaces* **2014**, *130*, 255.

[140] S. Mei, H. Wang, W. Wang, L. Tong, H. Pan, C. Ruan, Q. Ma, M. Liu, H. Yang, L. Zhang, Y. Cheng,

Y. Zhang, L. Zhao, P. K. Chu, *Biomaterials* **2014**, *35*, 4255.

[141] A. Roguska, A. Belcarz, M. Pisarek, G. Ginalska, M. Lewandowska, *Mater. Sci. Eng. C* **2015**, *51*, 158.

[142] P. J. Finley, R. Norton, C. Austin, A. Mitchell, S. Zank, P. Durham, *Antimicrob. Agents Chemother*. **2015**, *59*, 4734.

[143] Z. Peng, J. Ni, K. Zheng, Y. Shen, X. Wang, G. He, S. Jin, T. Tang, *Int. J. Nanomed.* **2013**, *8*, 3093.

[144] I. Izquierdo-Barba, J. M. Garcia-Martin, R. Alvarez, A. Palmero, J. Esteban, C. Perez-Jorge, D. Arcos, M. Vallet-Regí, *Acta Biomater*. **2015**, *15*, 20.

[145] W. Chen, Y. Liu, H. S. Courtney, M. Bettenga, C. M. Agrawal, J. D. Bumgardner, J. L. Ong, *Biomaterials* **2006**, *27*, 5512.

[146] W. Chen, S. Oh, A. P. Ong, N. Oh, Y. Liu, H. S. Courtney, M. Appleford, J. L. Ong, *J. Biomed. Mater. Res. A* **2007**, *82*, 899.

[147] A. Besinis, S. D. Hadi, H. R. Le, C. Tredwin, R. D. Handy, *Nanotoxicology* **2017**, *11*, 327.

[148] M. A. Surmeneva, A. A. Sharonova, S. Chernousova, O. Prymak, K. Loza, M. S. Tkachev, I. A. Shulepov, M. Epple, R. A. Surmenev, *Colloids Surf. B Biointerfaces* **2017**, 156, 104.

[149] C.-M. Xie, X. Lu, K.-F. Wang, F.-Z. Meng, O. Jiang, H.-P. Zhang, W. Zhi, L.-M. Fang, *ACS Appl. Mater. Interfaces* **2014**, *6*, 8580.

[150] G. A. Fielding, M. Roy, A. Bandyopadhyay, S. Bose, *Acta Biomater*. **2012**, *8*, 3144.

[151] Z. Geng, Z. Cui, Z. Li, S. Zhu, Y. Liang, Y. Liu, X. Li, X. He, X. Yu, R. Wang, X. Yang, *Mater. Sci. Eng. C* **2016**, *58*, 467.

[152] Z. Geng, R. Wang, X. Zhuo, Z. Li, Y. Huang, L. Ma, Z. Cui, S. Zhu, Y. Liang, Y. Liu, H. Bao, X. Li, Q. Huo, Z. Liu, X. Yang, *Mater. Sci. Eng. C* **2017**, *71*, 852.

[153] M. Kazemzadeh-Narbat, J. Kindrachuk, K. Duan, H. Jenssen, R. E. Hancock, R. Wang, *Biomaterials* **2010**, *31*, 9519.

[154] M. Kazemzadeh-Narbat, S. Noordin, B. A. Masri, D. S. Garbuz, C. P. Duncan, R. E. W. Hancock, R. Wang, *J. Biomed. Mater. Res. B Appl. Biomater*. **2012**, *100*, 1344.

[155] V. Alt, A. Bitschnau, J. Osterling, A. Sewing, C. Meyer, R. Kraus, S. A. Meissner, S. Wenisch, E. Domann, R. Schnettler, *Biomaterials* **2006**, *27*, 4627.

[156] S. Radin, J. T. Campbell, P. Ducheyne, J. M. Cuckler, *Biomaterials* **1997**, *18*, 777.

[157] H. Gautier, G. Daculsi, C. Merle, *Biomaterials* **2001**, 22, 2481.

[158] C. J. Pan, Y. X. Dong, Y. Y. Zhang, Y. D. Nie, C. H. Zhao, Y. L. Wang, *J. Orthop. Sci*. **2011**, *16*, 105.

[159] V. Uskokovic, C. Hoover, M. Vukomanovic, D.P. Uskokovic, T.A. Desai, *Mater. Sci. Eng. C Mater. Biol. Appl*. **2013**, *33*, 3362.

[160] M. Kazemzadeh-Narbat, B. F. Lai, C. Ding, J. N. Kizhakkedathu, R. E. Hancock, R. Wang, *Biomaterials* **2013**, *34*, 5969.

[161] C. Labay, J. M. Canal, M. Modic, U. Cvelbar, M. Quiles, M. Armengol, M. A. Arbos, F. J. Gil, C. Canal, *Biomaterials* **2015**, *71*, 132.

[162] C. Canal, M. Modic, U. Cvelbar, M. P. Ginebra, *Biomater. Sci*. **2016**, *4*, 1454.

[163] U. K. Marelli, F. Rechenmacher, T. R. Sobahi, C. Mas-Moruno, H. Kessler, *Front. Oncol.* **2013**, *3*, 222.

[164] P. Rocas, M. Hoyos-Nogues, J. Rocas, J. M. Manero, J. Gil, F. Albericio, C. Mas-Moruno, *Adv. Healthcare Mater*. **2015**, *4*, 1956.

[165] E. M. Hetrick, M. H. Schoenfisch, *Chem. Soc. Rev*. **2006**, *35*, 780.

[166] M. Zilberman, J. J. Elsner, *J. Controlled Release* **2008**, *130*, 202.

[167] Z. Wang, K. Wang, X. Lu, C. Li, L. Han, C. Xie, Y. Liu, S. Qu, G. Zhen, *Adv. Healthcare Mater.* **2015**, *4*, 927.

[168] L. Han, Z.-m. Wang, X. Lu, L. Dong, C.-m. Xie, K.-f. Wang, X.-l. Chen, Y.-h. Ding, L.-t. Weng, *Colloids Surf. B Biointerfaces* **2015**, *126*, 452.

[169] D. S. W. Benoit, K. S. Anseth, *Biomaterials* **2005**, *26*, 5209.

[170] M. Schuler, D. W. Hamilton, T. P. Kunzler, C. M. Sprecher, M. de Wild, D. M. Brunette, M. Textor, S. G. P. Tosatti, *J. Biomed. Mater. Res. Part B* **2009**, *91*, 517.

[171] B. F. Bell, M. Schuler, S. Tosatti, M. Textor, Z. Schwartz, B. D. Boyan, *Clin. Oral Implants Res.* **2011**, *22*, 865.

[172] N. M. Moore, N. J. Lin, N. D. Gallant, M. L. Becker, *Acta Biomater*. **2011**, *7*, 2091.

[173] W. N. Yin, F. Y. Cao, K. Han, X. Zeng, R. X. Zhuo, X. Z. Zhang, *J. Mater. Chem. B* **2014**, *2*, 8434.

[174] M. Pagel, A. G. Beck-Sickinger, *Biol. Chem.* **2017**, *398*, 3.

[175] J. M. Ageitos, A. Sánchez-Pérez, P. Calo-Mata, T. G. Villa, *Biochem. Pharmacol*. **2017**, *133*, 117.

[176] C. De La Fuente-Núñez, M. H. Cardoso, E. De Souza Cândido, O. L. Franco, R. E. W. Hancock, *Biochim. Biophys. Acta – Biomembr*. **2016**, *1858*, 1061.

[177] N. Strempel, J. Strehmel, J. Overhage, *Curr. Pharm. Des*. **2015**, *21*, 67.

[178] M. Riool, A. de Breij, J. W. Drijfhout, P. H. Nibbering, S. A. J. Zaat, *Front. Chem.* **2017,** *5*, 63.

[179] W. Lin, C. Junjian, C. Chengzhi, S. Lin, L. Sa, R. Li, W. Yingjun, *J. Mater. Chem. B* **2015**, *3*, 30.

[180] M. Godoy-Gallardo, C. Mas-Moruno, M. C. Fernández-Calderón, C. Pérez-Giraldo, J. M. Manero, F. Albericio, F. J. Gil, D. Rodriguez, *Acta Biomater*. **2014**, *10*, 3522.

[181] M. Godoy-Gallardo, C. Mas-Moruno, K. Yu, J. M. Manero, F. J. Gil, J. N. Kizhakkedathu, D. Rodriguez, *Biomacromolecules* **2015**, *16*, 483.

[182] M. Hoyos-Nogués, F. Velasco, M.- P. Ginebra, J. M. Manero, F. J. Gil, C. Mas-Moruno, *ACS Appl. Mater. Interfaces* **2017**, *9*, 21618.

[183] H. H. Tuson, D. B. Weibel, *Soft Matter* **2013**, *9*, 4368.

[184] M. Hoyos-Nogués, J. Buxadera-Palomero, M. P. Ginebra, J. M. Manero, F. J. Gil, C. Mas-Moruno, *Colloids Surf. B Biointerfaces* **2018**, *169*, 30.

[185] A. K. Muszanska, E. T. J. Rochford, A. Gruszka, A. A. Bastian, H. J. Busscher, W. Norde, H. C. Van Der Mei, A. Herrmann, *Biomacromolecules* **2014**, *15*, 2019.

[186] E. Yüksel, A. Karakeçili, T. T. Demirtas, M. Gümüsderelioglu, *Int. J. Biol. Macromol*. **2016**, *86*, 162.

[187] E. Jabbari, *Curr. Pharm. Des*. **2013**, *19*, 3391.

[188] F. R. Maia, S. J. Bidarra, P. L. Granja, C. C. Barrias, *Acta Biomater.* **2013**, *9*, 8773.

[189] J. K. Bronk, B. H. Russell, J. J. Rivera, R. Pasqualini, W. Arap, M. Hook, E. Magda Barbu, *Acta Biomater*. **2014**, *10*, 3354.

[190] M. Godoy-Gallardo, J. Guillem-Marti, P. Sevilla, J. M. Manero, F. J. Gil, D. Rodriguez, *Mater. Sci. Eng. C* **2016**, *59*, 524.

[191] S. Yuran, A. Dolid, M. Reches, *ACS Biomater. Sci. Eng*., DOI: 10.1021/acsbiomaterials.8b00885

[192] A. Ponche, M. Bigerelle, K. Anselme, *Proc. Inst. Mech. Eng. H* **2010**, *224*, 1471.

[193] R. A. Gittens, R. Olivares-Navarrete, Z. Schwartz, B. D. Boyan, *Acta Biomater.* **2014**, *10*, 3363.

[194] R. Harrison, *Science* **1911**, *34*, 279.

[195] P. Weiss, B. Garber, *Proc. Natl. Acad. Sci. USA* **1952**, *38*, 264.

[196] A. S. Curtis, M. Varde, *J. Nat. Cancer Res. Inst.* **1964**, *33*, 15.

[197] A. S. Curtis, *Eur. Cells Mater.* **2004**, *8*, 27.

[198] C. D. W. Wilkinson, *Eur. Cells Mater.* **2004**, *8*, 21.

[199] A. S. Curtis, C. D. Wilkinson, *J. Biomater. Sci. Polym. Ed.* **1998**, *9*, 1313.

[200] A. Curtis, C. Wilkinson, *Biomaterials* **1997**, *18*, 1573.

[201] S. Britland, H. Morgan, B. Wojiak-Stodart, M. Riehle, A. Curtis, C. Wilkinson, *Exp. Cell Res.* **1996**, *228*, 313.

[202] B. Wojciak-Stothard, A. S. Curtis, W. Monaghan, M. McGrath, I. Sommer, C. D. Wilkinson, *Cell Motility Cytoskeleton* **1995**, *31*, 147.

[203] B. Wojciak-Stothard, Z. Madeja, W. Korohoda, A. Curtis, C. Wilkinson, *Cell Biol. Int.* **1995**, *19*, 485.

[204] P. Clark, P. Connolly, A. S. Curtis, J. A. Dow, C. D. Wilkinson, *Development* **1990**, *108*, 635.

[205] P. Clark, P. Connolly, A. S. Curtis, J. A. Dow, C. D. Wilkinson, *Development* **1987**, *99*, 439.

[206] P. Clark, P. Connolly, A. S. Curtis, J. A. Dow, C. D. Wilkinson, *J. Cell. Sci.* **1991**, *99 (Pt1)*, 73.

[207] C. Vieu, F. Carcenac, A. Pépin, Y. Chen, M. Mejias, A. Lebib, L. Manin-Ferlazzo, L. Couraud, H. Launois, *Appl. Surf. Sci.* **2000**, *164*, 111.

[208] F. A. Denis, P. Hanarp, D. S. Sutherland, J. Gold, C. Mustin, P. G. Rouxhet, Y. F. Dufrêne, *Langmuir* **2002**, *18*, 19.

[209] P. Hanarp, D. Sutherland, J. Gold, B. Kasemo, *Nanostruct. Mater* **1999**, *12*, 429.

[210] S. Affrossman, M. Stamm, *Colloid Polym. Sci.* **2000**, *278*, 888.

[211] S. Affrossman, R. Jerome, S. A. O'Neill, T. Schmitt, M. Stamm, *Colloid Polym. Sci.* **2000**, *278*, 993.

[212] S. Krishnamoorthy, C. Hibert, M. Liley, A. Meister, M. Dalby, R. Oreffo, J. Brugger, R. Pugin, H. Heinzelmann, C. Hinderling, In *International Conference on Nanoscience and Technology ICN&T;* **2006**.

[213] S. Krishnamoorthy, R. Pugin, M. Liley, M. J. Dalby, R. Oreffo, H. Heinzelmann, J. Brugger, C. Hinderling, In *Biosurf. VI-Tissue-Surface Interaction;* **2005**.

[214] M. Dalby, M. Riehle, H. Johnstone, S. Affrossman, A. Curtis, *Biomaterials* **2002**, *23*, 2945.

[215] E. K. Yim, R. M. Reano, S. W. Pang, A. F. Yee, C. S. Chen, K. W. Leong, *Biomaterials* **2005**, *26*, 5405.

[216] A. S. G. Curtis, N. Gadegaard, M. J. Dalby, M. O., Riehle, C. D. W. Wilkinson, G. Aitchison, *NanoBioscience, IEEE Transactions* **2004**, *3*, 61.

[217] N. Gadegaard, S. Thoms, D. S. Macintyre, K. Mcghee, J. Gallagher, B. Casey, C. D. W. Wilkinson, *Microelectronic Engineering* **2003**, *67-68*, 162.

[218] F. A. Denis, P. Hanarp, D. S. Sutherland, Y. F. Dufrene, *Nano Lett.* **2002**, *2*, 1419.

[219] E. M. Hur, K. T. Kim, *Cell Signal* **2002**, *14*, 397.

[220] J. Huang, S. V. Grater, F. Corbellini, S. Rinck, E. Bock, R. Kemkemer, H. Kessler, J. Ding, J. P. Spatz, *Nano Lett.* **2009**, *9*, 1111.

[221] R. J. McMurray, N. Gadegaard, P. M. Tsimbouri, K. V. Burgess, L. E. McNamara, R. Tare, K. Murawski, E. Kingham, R. O. Oreffo, M. J. Dalby, *Nat. Mater.* **2011**, *10*, 637.

[222] M. J. Dalby, N. Gadegaard, R. Tare, A. Andar, M. O. Riehle, P. Herzyk, C. D. Wilkinson, R. O. Oreffo, *Nat. Mater.* **2007**, *6*, 997.

[223] S. Krishnamoorthy, R. Pugin, J. Brugger, H. Heinzelmann, A. C. Hoogerwerf, C. Hinderling, *Langmuir* **2006**, *22*, 3450.

[224] M. J. Dalby, D. McCloy, M. Robertson, H. Agheli, D. Sutherland, S. Affrossman, R. O. Oreffo, *Biomaterials* **2006**, *27*, 2980.

[225] R. K. Silverwood, P. G. Fairhurst, T. Sjöström, F. Welsh, Y. Sun, G. Li, B. Yu, P. S. Young, B. Su, R. M. Meek, M. J. Dalby, P. M. Tsimbouri, *Adv. Healthc. Mater.* **2016**, *5*, 947.

[226] T. Sjostrom, L. E. McNamara, L. Yang, M. J. Dalby, B. Su, *ACS Appl. Mater. Interfaces* **2012**, *4*, 6354.

[227] L. E. McNamara, T. Sjöström, K. E. Burgess, J. J. Kim, E. Liu, S. Gordonov, P. V. Moghe, R. M. Meek, R. O. Oreffo, B. Su, M. J. Dalby, *Biomaterials* **2011**, *32*, 7403.

[228] T. Sjostrom, N. Fox, B. Su, *Nanotechnol.* **2009**, *20*, 135305.

[229] N. Gadegaard, M. J. Dalby, M. O. Riehle, A. S. G. Curtis, S. Affrossman, *Adv. Mater.* **2004**, *16*, 1857.

[230] C. C. Berry, M. J. Dalby, R. O. Oreffo, D. McCloy, S. Affrosman, *J. Biomed. Mater. Res. A* **2006**, *79*, 431.

[231] H. M. Birch, *Nature* **2007**, *446*, 937.

[232] A. Mata, E. J. Kim, C. A. Boehm, A. J. Fleischman, G. F. Muschler, S. Roy, *Biomaterials* **2009**, *30*, 4610.

[233] M. J. Dalby, M. O. Riehle, H. Johnstone, S. Affrossman, A. S. Curtis, *Cell Biol. Int.* **2004**, *28*, 229.

[234] L. E. McNamara, T. Sjöström, K. Seunarine, R. D. Meek, B. Su, M. J. Dalby, *J. Tissue Eng.* **2014**, *5*, 2041731414536177.

[235] A. I. Teixeira, G. A. Abrams, P. J. Bertics, C. J. Murphy, P. F. Nealey, *J. Cell Sci.* **2003**, *116*, 1881.

[236] R. K. Das, O. F. Zouani, C. Labrugere, R. Oda, M. C. Durrieu, *ACS Nano* **2013**, *7*, 3351.

[237] E. A. Cavalcanti-Adam, T. Volberg, A. Micoulet, H. Kessler, B. Geiger, J. P. Spatz, *Biophys. J.* **2007**, *92*, 2964.

[238] J. Yang, L. E. McNamara, N. Gadegaard, E. V. Alakpa, K. V., Burgess, R. M. Meek, M. J. Dalby, *ACS Nano* **2014**, *8*, 9941.

[239] J. Malmstrom, J. Lovmand, S. Kristensen, M. Sundh, M. Duch, D. S. Sutherland, *Nano Lett.* **2011**, *11*, 2264.

[240] M. J. Biggs, R. G. Richards, N. Gadegaard, C. D. Wilkinson, R. O. Oreffo, M. J. Dalby, *Biomaterials* **2009**, *30*, 5094.

[241] C. S. Buensuceso, D. Woodside, J. L. Huff, G. E. Plopper, T. E. O'Toole, *J. Cell Sci.* **2001**, *114*, 1691.

[242] M. J. Dalby, A. Hart, S. J. Yarwood, *Biomaterials* **2008**, *29*, 282-289.

[243] N. Q. Balaban, U. S. Schwarz, D. Riveline, P. Goichberg, G. Tzur, I. Sabanay, D. Mahalu, S. Safran, A. Bershadsky, L. Addadi, B. Geiger, *Nat. Cell Biol.* **2001**, *3*, 466.

[244] T. Shemesh, B. Geiger, A. D. Bershadsky, M. M. Kozlov, *Proc. Natl. Acad. Sci. U. S. A.* **2005**, *102*, 12383.

[245] A. J. Engler, S. Sen, H. L. Sweeney, D. E. Discher, *Cell* **2006**, *126*, 677.

[246] R. McBeath, D. M. Pirone, C. M. Nelson, K. Bhadriraju, C. S. Chen, *Dev. Cell* **2004**, *6*, 483.

[247] K. A. Kilian, B. Bugarija, B. T. Lahn, M. Mrksich, *Proc. Natl. Acad. Sci. U. S. A.* **2010**, *107*, 4872.

[248] N. A. Patankar, *Langmuir* **2004**, *20*, 8209–8213.

[249] M. Yamamoto, N. Nishikawa, H. Mayama, Y. Nonomura, S. Yokojima, S. Nakamura, K. Uchida, *Langmuir* **2015**, *31*, 7355.

[250] J. Ma, Y. Sun, K. Gleichauf, J. Lou, Q. Li, *Langmuir* **2011**, *27*, 10035.

[251] J. K. Oh, X. Lu, Y. Min, L. Cisneros-Zevallos, M. Akbulut, *ACS Appl. Mater. Interfaces* **2015**, *7*, 19274.

[252] F. Hizal, N. Rungraeng, J. Lee, S. Jun, H. J. Busscher, H. C. Van der Mei, C. H. Choi, *ACS Appl. Mater. Interfaces* **2017**, *9*, 12118.

[253] W. Choi, E. P. Chan, J. H. Park, W. G. Ahn, H. W. Jung, S. Hong, J. S. Lee, J. Y. Han, S. Park, D. H. Ko, J. H. Lee, *ACS Appl. Mater. Interfaces* **2016**, *8*, 31433.

[254] E. Beltrán-Partida, B. Valdez-Salas, M. Curiel-Álvarez, S. Castillo-Uribe, A. Escamilla, N. Nedev, *Mater. Sci. Eng.* **2017**, *76*, 59.

[255] C. Lüdecke, M. Roth, W. Yu, U. Horn, J. Bossert, K. D. Jandt, *Colloids Surf. B: Biointerfaces* **2016**, *145*, 617.

[256] J. Pang, T. Sjöström, D. Dynmock, B. Su, *Bioinspired, Biomimetic and Nanobiomaterials* **2013**, *2*, 117.

[257] S. Kim, Y. Zhou, J. D. Cirillo, A. A. Polycarpou, H. Liang, *J. Appl. Phys*. **2015**, *117*, 155302.

[258] E. Dayyoub, E. Belz, N. Dassinger, M. Keusgen, U. Bakowsky, *Phys. Status Solidi A* **2011**, *208*, 1279.

[259] C. Serrano, L. García-Fernández, J. P. Fernández-Blázquez, M. Barbeck, S. Ghanaati, R. Unger, J. Kirkpatrick, E. Arzt, L. Funk and P. Turón, *Biomaterials* **2015**, *52*, 291.

[260] S. Liu, L. Wei, L. Hao, N. Fang, M. W. Chang, R. Xu, Y. Yang, Y. Chen, *ACS Nano* **2009**, *3*, 3891.

[261] E. P. Ivanova, J. Hasan, H. K. Webb, V. K. Truong, G. S. Watson, J. A. Watson, V. A. Baulin, S. Pogodin, J. Y. Wang, M. J. Tobin, C. Löbbe, R. J. Crawford, *Small* **2012**, *8*, 2489.

[262] S. Pogodin, J. Hasan, V. A. Baulin, H. K. Webb, V. K. Truong, T. H. Phong Nguyen, V. Boshkovikj, C. J. Fluke, G. S. Watson, J. A. Watson, R. J. Crawford, E. P. Ivanova, *Biophys. J.* **2013**, *104*, 835.

[263] S. M. Kelleher, O. Habimana, J. Lawler, B. O'Reilly, S. Daniels, E. Casey, A. Cowley, *ACS Appl. Mater. Interfaces* **2015**, *8*, 14966.

[264] A. Elbourne, R. J. Crawford, E. P. Ivanova, *J. Colloid Interface Sci*. **2017**, *508*, 603.

[265] A. Tripathy, P. Sen, B. Su, W. H. Briscoe, *Adv. Colloid Interface Sci*. **2017**, *248*, 85.

[266] D. E. Mainwaring, S. H. Nguyen, H. Webb, T. Jakubov, M. Tobin, R. N. Lamb, A. H. F. Wu, R. Marchan, R. J. Crawford, E. P. Ivanova, *Nanoscale* **2016**, *8*, 6527.

[267] V. K. Truong, N. M. Geeganagamage, V. A. Baulin, J. Vongsvivut, M. J. Tobin, P. Luque, R. J. Crawford, E. P. Ivanova, *Appl. Microbiol. Biotechnol*. **2017**, 101, 4683.

[268] F. Viela, I. Navarro-Baena, J. J. Hernández, M. R. Osorio, I. Rodríguez, *Bioinsp. Biomim*. **2018**, *13*, 026011.

[269] X. Li, G. S. Cheung, G. S. Watson, J. A. Watson, S. Lin, L. Schwarzkopf, D. W. Green, *Nanoscale* **2016**, *8*, 18860.

[270] M. J. Hayes, T. P. Levine, R. H. Wilson, *J. Insect. Sci*. **2016**, 16, 1.

[271] E. P. Ivanova, J. Hasan, H. K. Webb, G. Gervinskas, S. Juodkazis, V. K. Truong, A. H. F. Wu, R. N. Lamb, V. A. Baulin, G. S. Watson, J. A. Watson, D. E. Mainwaring, R. J. Crawford, *Nat. Commun*. **2013**, *4*, 2838.

[272] H. Hu, V. S. Siu, S. M. Gifford, S. Kim, M. Lu, P. Meyer, G. A. Stolovitzky, *Appl. Phys. Lett*. **2017**, *111*, 253701.

[273] D. P. Linklater, H. K. D. Nguyen, C. M. Bhadra, S. Juodkazis, E. P. Ivanova, *Nanotechnology* **2017**, *28*, 245301.

[274] A. Susarrey-Arce, I. Sorzabal-Bellido, A. Oknianska, F. McBride, A. Beckett, J. Gardeniers, R. Raval, R. Tiggelaar, Y. D. Fernandez, *J. Mater. Chem. B* **2016**, *4*, 3104.

[275] L. E. Fisher, Y. Yang, M. F. Yuen, W. Zhang, A. H. Nobbs, B. Su, *Biointerphases* **2016**, *11*, 011014.

[276] P. W. May, M. Clegg, T. A. Silva, H. Zanin, O. Fatibello-Filho, V. Celorrio, D. J. Fermin, C. C. Welch, G. Hazell, L. Fisher, A. Nobbs, B. Su. *J. Mater. Chem. B* **2016**, *4*, 5737.

[277] G. Hazell, P. W. May, P. Taylor, A. H. Nobbs, C. C. Welch, B. Su, *Biomater. Sci*. **2018**, *6*, 1424.

[278] T. Diu, N. Faruqui, T. Sjöström, B. Lamarre, H. F. Jenkinson, B. Su, M. G. Ryadnov, *Sci. Rep.* **2014**, *4*, 7122.

[279] C. M. Bhadra, V. Khanh Truong, V. T. H. Pham, M. Al Kobaisi, G. Seniutinas, J. Y. Wang, S. Juodkazis, R. J. Crawford, E. P. Ivanova, *Sci. Rep*. **2015**, *5*, 16817.

[280] Y. Cao, B. Su, S. Chinnaraj, S. Jana, L. Bowen, S. Charlton, P. Duan, N. S. Jakubovics, J. Chen, *Sci. Rep*. **2018**, *8*, 1071.

[281] A. Jaggessar, A. Mathew, H. Wang, T. Tesfamichael, C. Yan, P. K. D. V Yarlagadda, *J. Mech. Behav. Biomed. Mater*. **2018**, *80*, 311.

[282] C. Sengstock, M. Lopian, Y. Motemani, A. Borgmann, C. Khare, P. J. S. Buenconsejo, T. A. Schildhauer, A. Ludwig, M. Köller, *Nanotechnology* **2014**, *25*, 195101.

[283] J. Hasan, S. Jain, K. Chatterjee, *Sci Rep* **2017**, *7*, 41118.

[284] T. Sjöström, A. H Nobbs, B. Su, *Mater. Lett.* **2016**, *167*, 22.

[285] M. N. Dickson, E. I. Liang, L. A. Rodriguez, N. Vollereaux, A. F. Yee, *Biointerphases* **2015**, *10*, 021010.

[286] K. Minoura, M. Yamada, T. Mizoguchi, T. Kaneko, K. Nishiyama, M. Ozminskyj, T. Koshizuka, I. Wada, T. Suzutani, *PLoS ONE* **2017**, 12, e0185366.

[287] F. Viela, I. Navarro-Baena, J. J. Hernández, M. R. Osorio, I. Rodrigues, *Bioinspir. Biomim.* **2018**, *13*, 026011.

[288] G. Hazell, L. E. Fisher, W. A. Murray, A. H. Nobbs, B. Su, *J. Colloid Interface Sci*. **2018**, *528*, 389.

[289] Y. Jang, W. T. Choi, C. T. Johnson, A. J. García, P. M. Singh, V. Breedveld, D. W. Hess, J. A. Champion, *ACS Biomater. Sci. Eng*. **2018**, *4*, 90.

[290] J. Hasan, S. Jain, R. Padmarajan, S. Purighalla, V. K. Sambandamurthy, K. Chatterjee, *Mater. Des*. **2018**, *140*, 332.

[291] P. A. Nistor, P. W. May, *J. R. Soc. Interface* **2017**, *14*, 20170382.

[292]K. Kapat , P. P. Maity, A. P. Rameshbabu, P. K. Srivas, P. Majumdar, S. Dhara, *J. Mater. Chem. B* **2018**, *6*, 2877.

[293] V. Goriainov, G. Hulsart-Billstrom, T. Sjostrom, D. G. Dunlop, B. Su, R. O. C. Oreffo, *Front. Bioeng. Biotechnol*. **2018**, *6*, 44.

[294] M. Fernandez-Fairen, A. Torres, A. Menzie, D. Hernandez-Vaquero, J. M. Fernandez-Carreira, A. Murcia-Mazon, E. Guerado, L. Merzthal, *Open Orthop. J*. **2013**, *7*, 227.

[295] X. Wang, T. Lu, J. Wen, L. Xu, D. Zeng, Q. Wu, L. Cao, S. Lin, X. Liu, X. Jiang, *Biomaterials* **2016**, *83*, 207.

[296] V. T. Pham, V. K. Truong, A. Orlowska, S. Ghanaati, M. Barbeck, P. Booms, A. J. Fulcher, C. M. Bhadra, R. Buividas, V. Baulin, C. J. Kirkpatrick, P. Doran, D. E. Mainwaring, S. Juodkazis, R. J. Crawford, E. P. Ivanova, *ACS Appl. Mater. Interfaces* **2016**, *8*, 22025.

[297] P. M. Tsimbouri, L. Fisher, N. Holloway, T. Sjostrom, A. H. Nobbs, R. M. Meek, B. Su B, M. J. Dalby, *Sci. Rep*. **2016**, *6*, 36857.

[298] R. Fraioli, P. M. Tsimbouri, L. E. Fisher, A. H. Nobbs, B. Su, S. Neubauer, F. Rechenmacher, H. Kessler, M. P. Ginebra, M. J. Dalby, J. M. Manero, C. Mas-Moruno, *Sci. Rep.* **2017**, *7*, 16363.

[299] J. N. Roberts, J. K. Sahoo, L. E. McNamara, K. V. Burgess, J. Yang, E. V. Alakpa, H. J. Anderson, J. Hay, L.-A. Turner, S. J. Yarwood, M. Zelzer, R. O. C. Oreffo, R. V. Ulijn, M. J. Dalby, *ACS Nano* **2016**, *10*, 6667.

[300] M.-H. Xiong, Y.-J. Li, Y. Bao, X.-Z. Yang, B. Hu, J. Wang, *Adv. Mater.* **2012**, *24*, 6175.

[301] G. D. Wright, *Nat. Prod. Rep*. **2017**, *34*, 694.

[302] O. Genilloud, *Nat. Prod. Rep*. **2017**, *34*, 1203.

[303] M. K. Kim, A. Zhao, A. Wang, Z. Z. Brown, T. W. Muir, H. A. Stone, B. L. Bassler, *Nature Microbiol*. **2017**, *2*, 17080.